Ocean Engineering 355 (2026) 124918

Contents lists available at ScienceDirect

Ocean Engineering

journal homepage: www.elsevier.com/locate/oceaneng

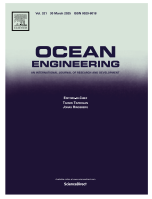

Accurately forecasting saltwater intrusion through navigation locks requires nautical traffic simulation modelling

Floor P. Bakker [a,*], Jikke W.E. de Ruiter [a], Arne J. van der Hout [a,b], Mark van Koningsveld [a,c]

[a] Delft University of Technology, Faculty of Civil Engineering and Geosciences, PO Box 5048, 2600 GA, Delft, the Netherlands
[b] Deltares, Boussinesqweg 1, 2629 HV, Delft, the Netherlands
[c] Van Oord Dredging and Marine Contractors B.V, PO Box 8574, 3009 AN, Rotterdam, the Netherlands

ARTICLE INFO

Keywords:
Saltwater intrusion
Vessel delays
Navigation locks
Closed systems
Nautical traffic simulation
Lock exchange models

ABSTRACT

Navigation locks enable vessel transit between separated water bodies but also induce water exchange, leading to saltwater intrusion. During droughts, operational strategies that limit this intrusion cause vessel delays. Consequently, accurate estimation of the salt intrusion is essential for optimising these strategies. Current analytical lock exchange models, such as the Sea Lock Formulation, are a suitable and computationally efficient option for this purpose. However, the performance of these models relies on scarce gate-status data of the lock operation. To overcome this challenge, we present a novel method integrating the Sea Lock Formulation with the nautical traffic model OpenTNSim to derive time-varying lock operation parameters from accessible vessel data. This approach uniquely enables simultaneous evaluation of mitigation strategies on both saltwater intrusion and traffic performance. Applied to the world's largest lock at IJmuiden, the model is validated against measured salt concentration and operation records. When forecasting, our method significantly improves the accuracy of the analytical models, reducing long-term salt intrusion errors from +22.2% to −2.6%. This marks a critical advancement toward a systematic exploration of tradeoffs between hydraulic and nautical objectives, enabling, for the first time, integrated lock management strategies that balance hydraulic protection with nautical efficiency in closed waterway systems.

1. Introduction

Navigation locks form critical links in waterborne transport systems, enabling the passage of vessels past hard structures, such as dams and weirs. These structures regulate water levels for navigation, store freshwater, and separate water bodies with different salinities. Lock operation, however, inevitably causes water exchange—through density-driven currents when gates are open (Vrijburcht, 1991), levelling, and vessel movement—leading to net water loss in the water body with higher water levels and, where salinity gradients exist, saltwater intrusion into the fresher water body. Under average conditions, the freshwater losses can be replenished by upstream discharge and local precipitation, which also flush out saltwater. During droughts, however, freshwater shortages can arise when demand—for consumption and saltwater flushing—exceeds supply with internal freshwater storage depleted. The low dynamic water system behind the lock typically requires substantial freshwater for flushing (Biemond et al., 2024).

Water exchange through navigation locks can be reduced by infrastructural measures, such as water-saving basins (Jongeling, 2004; Xu et al., 2023; Zhu et al., 2023)—although counterproductive for mitigating saltwater intrusion—as well as water screens (Uittenbogaard and Cornelisse, 2011), pneumatic barriers or bubble screens (Abraham and Van der Burgh, 1964; Abraham et al., 1973; Uittenbogaard and Cornelisse, 2011; Uittenbogaard et al., 2015; O'Mahoney et al., 2024), sills (Mausshardt and Singleton, 1995; Keetels et al., 2011; Uittenbogaard and Cornelisse, 2011), salt traps (Van der Kuur, 1985; Vrijburcht, 2000a), flushing (Van der Kuur, 1985; Kerstma et al., 1994; Mausshardt and Singleton, 1995; Vrijburcht, 2000a; Uittenbogaard and Cornelisse, 2011), saltwater substitution (PIANC, 1986; Kerstma et al., 1994; Vrijburcht, 2000a; O'Mahoney et al., 2023), and selective withdrawal (Jirka, 1979; Jirka and Katavola, 1979; de Fockert et al., 2022). Above measures can be combined with operational salt intrusion mitigation strategies, such as clustering vessels or reducing gate-open durations (PIANC, 2021). However, these can significantly impact water-

* Corresponding author.
E-mail address: F.P.Bakker@tudelft.nl (F.P. Bakker).

https://doi.org/10.1016/j.oceaneng.2026.124918
Received 15 December 2025; Received in revised form 14 February 2026; Accepted 1 March 2026
Available online 20 March 2026

borne transport by increasing vessel delays and reducing safety. With climate change projected to increase the frequency of prolonged droughts (Jones et al., 2024; Lee et al., 2024), maintaining both freshwater availability and waterborne transport functionality becomes a major challenge (Vinke et al., 2022, 2024; Bakker et al., 2025). Accurate estimation of freshwater losses and saltwater intrusion as a function of the lock operation is therefore essential to design lock complexes and operation strategies that balance freshwater availability with efficient navigation over extended periods.

Various useful methods to estimate lock exchange fluxes have been presented in literature. Research has generally focused on modelling the density-driven exchange using physical and analytical methods (Keulegan, 1957; Benjamin, 1968). One of the first numerical studies was performed by Kao et al. (1977) using a hydrostatic model. At present, state-of-the-art, non-hydrostatic, Eulerian (mesh-based) Computational Fluid Dynamics (CFD) models are most commonly used. They can accurately predict the speed and shape of the density-driven current, thereby estimating the exchange rate of the lock chamber. Various implementations exist. First, they discretise the incompressible Navier-Stokes equations differently through the Boussinesq approximation. Examples are the Finite-Element Method (FEM) (Rossa and Coutinho, 2013), Lattice Boltzmann Method (LBM) (Ottolenghi et al., 2018), Finite Volume Method (FVM) (Lai et al., 2010), and Finite Difference Method (FDM) (Lesshafft et al., 2011). Second, they use alternative turbulence models, such as Direct Numerical Simulation (DNS) (Härtel et al., 1997; Zhao et al., 2019), Large-eddy simulation (LES) (Constantinescu, 2014; Pelmard et al., 2018) and Reynolds-averaging (RANS) (e.g., k-epsilon Stancanelli et al., 2018). Third and last, they use other mesh types (Bombardelli et al., 2009), time integration (e.g., explicit and implicit), and different (wall) boundary conditions. Each method has its requirements, strengths and weaknesses, reflecting a trade-off between accuracy and computation efficiency. The numerical models are versatile and are also used in modelling exchange flows in estuaries, i.e., Chen et al. (2012), Kim and Park (2012), Geyer et al. (2005), and MacCready et al. (2018). Recent developments in CFD have enabled the study of other lock exchange fluxes, such as levelling through filling/emptying systems (Stockstill and Berger, 2009; Thorenz and Strybny, 2012; Calvo Gobbetti, 2013; Battiston et al., 2020), sailing vessels through lock chambers (De Loor et al., 2013; Henn, 2013; Lindberg et al., 2013; Vergote et al., 2013; Wang and Zou, 2013, 2014; Toxopeus and Bhawsinka, 2013; Mucha, 2025), and lock exchange with bubble screens (van der Ven et al., 2018; Oldeman et al., 2020) and flushing discharges (Van Beek, 2021).

Alternatively to CFD, Langrangian (meshless) Smoothed Particle Hydrodynamics (SPH) methods are applied (Basser et al., 2017). These methods consider particles individually and are therefore often more computationally expensive than Eulerian CFD methods (Pozorski and Olejnik, 2023). In contrast, faster grid-based methods exist that solve the simpler Shallow Water Equations (SWE) or Depth-averaged Navier-Stokes equations (Kolar et al., 2009; Hatcher et al., 2012).

The above numerical methods can be applied in less computationally demanding two-dimensional simulations, such as CFD (Keetels et al., 2011), SPH (Shao, 2011; Ghasemi V. et al., 2013), and SWE (Hatcher et al., 2012), as well as one-dimensional simulations (e.g., two-layer SWE Hatcher and Vasconcelos, 2013). However, even with dimensionality reduction and model simplification, these methods incur substantial computational costs. Given the virtually endless combinations of initial boundary conditions for each lock operation—i.e., water levels, salt concentrations, gate-open durations, occupation volumes of exiting and entering vessels, and the lock chamber dimensions–the numerical methods are not deemed suitable to estimate water exchange fluxes through navigation locks over extended periods involving large numbers of lock cycles. Instead, the methods would be highly suitable for testing specific lock designs and calibrating simpler hydrodynamic lock exchange models.

As a promising alternative to numerical models, rapid analytical models can be used to estimate lock exchange fluxes. These simple volume-balance models discretise the lock operation into four phases that together constitute a full lock cycle: levelling to sea, gate-open at sea, levelling to the canal, gate-open at the canal. For each phase, the models estimate the water and salt exchange mass fluxes for density-driven currents, entering and exiting vessel volumes, and levelling prisms. Examples are models by Parchure et al. (2000) and Jongeling (2003), which were applied to the Panama Canal Locks (see also applications by Marin et al., 2010,Rabelo et al., 2014 and Wijsman, 2013). These models simplify the density-driven current by using an exchange coefficient that specifies the percentage of water exchanged in the lock chamber. Therefore, extensive calibration is required based on detailed salinity measurements.

A more detailed analytical model is the General Salt Intrusion Model of Uittenbogaard (2010) in WANDA-locks[1]. Rather than exchange coefficients, this method uses a semi-empirical relation to estimate the initial speed of the density-driven current and the subsequent volume exchange (van der Burgh and de Vos, 1962; Vrijburcht, 2000b). WANDA-locks can rapidly model flows through pipes of levelling systems, where the General Salt Intrusion Model accounts for the various salt exchange fluxes of density-driven currents, levelling, flushing, ships and mitigation measures, such as bubble screens. Although WANDA-locks has been thoroughly validated by measurement campaigns and three-dimensional numerical models (De Groot- Wallast and Vreeken, 2016), its application is complex as it requires large amounts of detailed data (Weiler et al., 2019). To overcome this issue, the Sea Lock Formulation (ZSF) has been developed (Weiler et al., 2026) (*in Dutch: Zeesluisformulering*), which contains algorithms inspired by the General Salt Intrusion Model. It can be run in two modes: a detailed phase-wise mode, which, like WANDA-Locks, runs through a series of lock operation phases with varying properties, or a more practically-oriented lock cycle-averaged mode, in which periodically identical lock cycles are assumed. The phase-wise mode can handle phase-varying boundary conditions, namely gate-open durations, salt concentrations and water levels at both harbours, and vessel volumes. In contrast, the cycle-average application assumes periodically lock cycle-averaged conditions, of which the gate-open duration can be calibrated using two factors: one factor to correct for the average gate-open duration to a representative value for the density-driven current, and another to account for the asymmetry of gate-open durations at both sides of the lock. The factors can strongly influence the accuracy of the cycle-averaged results and are therefore often determined through cross-model calibration with the phase-wise modelling results.

Analytical models are deemed most suitable for assessing the impact of lock operation on freshwater shortage, as they produce fast and plausible estimates of exchange fluxes under lock operation-varying boundary conditions. In fact, these models are commonly used at a systemic level to implement infrastructural countermeasures to limit saltwater intrusion (Weiler, 2018), and to optimise lock complex designs for saltwater intrusion (Jongeling, 2004). In addition, the output of the analytical models can be applied to numerical models that estimate saltwater intrusion in the system behind the lock—e.g., Delft3D (Jongeling, 2008)—to assess its impact on the freshwater users.

To date, the confidence in the performance of analytical models mainly builds upon experience gained with earlier models, as they employ similar fundamental formulations to represent the governing physical processes. Intercomparison among models has further strengthened confidence in the calculated salt intrusion. Nevertheless, formal validation against field measurements remains limited due to the lack of real-world data. The recent study by Weiler et al. (2026) with the ZSF constitutes the only published validation, covering a relatively short period and a small lock chamber. In addition, specifically for the application of the ZSF, lock operation data, particularly gate-open durations, are required for reliable results. These data are scarce and difficult to predict for future scenario analyses involving different lock operation strategies,

[1] https://www.deltares.nl/en/software-and-data/products/wanda-software

evolving vessel fleets and traffic intensities, and new lock chambers. This was illustrated by the study of Vuik and Lambregts (2023) for a new lock chamber at the Terneuzen Lock Complex.

In this paper, we address the above knowledge gaps by comparing the performance of analytical models in forecasting salt intrusion mass fluxes. For this purpose, we focus on the ZSF, which is expected to provide the most realistic and technically robust estimates among available analytical models. To confirm the reliability of the method, we validate the predicted salt mass fluxes by the ZSF against estimations based on recently collected data by Deltares (2023) of gate-open statuses, vessel passages, and water levels, conductivities and temperatures at the newly built Sea Lock IJmuiden, the world's largest lock by surface area, between February and March of 2023. To quantify the forecasting performance of the ZSF, we compare the results of its two modes—cycle-averaged and phase-wise—applied without prior site-specific calibration, reflecting the conditions of a future scenario. Here, to overcome the practical challenges in setting up a phase-wise model—specifically, the need for detailed gate-open status data—we demonstrate the use of a nautical traffic model that estimates gate-open durations from better accessible and predictable vessel data. For this, we use the nautical traffic simulation library of OpenTNSim (van Koningsveld and den Uijl, 2019; Baart et al., 2022; Bakker et al., in prep.).

The paper is structured as follows. Section 2 introduces the case study, followed by Section 3 elaborating on the workflow. In this section, we first quantify the salt intrusion mass fluxes using the measurement campaign data. Second, based on the same dataset, we derive best-guess input parameters for the lock cycle-averaged and phase-wise models. Third, noting that data availability may be limited when forecasting, we assimilate time-varying gate-open time and vessel volume data, using OpenTNSim, which resolves lock operations based on more accessible and predictable vessel passage data. Fourth, using the above data, we validate the salt intrusion mass fluxes predicted by ZSF for each phase individually. Fifth and finally, we compare the long-term salt intrusion forecasts obtained from the following model applications, all without prior site-specific calibration: (1) lock cycle-averaged with steady hydrodynamic conditions, (2) lock cycle-averaged with periodically varying hydrodynamic conditions, (3) phase-wise with observed gate-open durations; and (4) phase-wise with gate-open durations assimilated using OpenTNSim. The results are presented in Section 4 and discussed in Section 5, followed by the conclusions in Section 6.

2. Case study

2.1. The IJmuiden lock complex

The IJmuiden Lock Complex separates the North Sea Canal (NSC)–Amsterdam-Rhine Canal (ARC) system (in Dutch: *Noordzeekanaal (NZK)–Amsterdam-Rijnkanaal (ARK) systeem*) from the North Sea (Fig. 1). This canal system was built to create a fast navigable connection between the North Sea, the Port of Amsterdam (PoA) and the Rhine and Waal Rivers, which form the inland water transport link to other seaports, such as the Port of Rotterdam, and the hinterland of Western Europe. For water management purposes, the NSC's target water level is set at −0.45 m Amsterdam Ordnance Datum (NAP) (in Dutch: *Normaal Amsterdams Peil*)—approximately equal to Mean Sea Level (MSL)—with little slack (−0.35 to −0.55 m). This target level ensures the following system functions:

1. Discharge of excess water from surrounding polders—low-lying areas below sea level, enclosed by dikes,
2. Navigation of nautical traffic through locations with height and depth restrictions, including the bridges of the Amsterdam canals for cruise boats, and, for cargo vessels, the tunnel roofs, bridges, and lift gates and sills of locks;
3. Flood protection of the hinterland, including the city of Amsterdam and its Port (Rijkswaterstaat, 2023).

To facilitate this, the IJmuiden Lock Complex comprises a discharge sluice and five navigational locks that enable the passage of inland vessels, and seagoing nautical traffic (Fig. 2(a) and (b)). The complex is also part of the primary flood defence of the Netherlands, and separates salty seawater of the North Sea with a salt concentration of 27.8–35.3 kgm^{-3} (Buschman et al., 2017) from the hinterland system's freshwater that is required for drinking water, agriculture, industry, and ecology (Fig. 1). Through lock operation, salt intrudes into the NSC, producing a stratified distribution ranging from brackish to saline water. Brackish water—above the chloride concentration limit of 0.28 kgm^{-3} for water intake stations and drinking water production—normally reaches up to 5 km from the entrance of the ARC (Buschman et al., 2017), close to the measurement location (Fig. 1). In the NSC, salt concentration vary between 3.6–21.6 kgm^{-3} (Buschman et al., 2017). Salt is primarily removed through discharging brackish water through the discharge sluice. Together with the water exchange caused by the operation of the navigation locks, this often leads to salt concentrations on the seaside of the lock complex being lower than in the North Sea.

The largest navigation lock of the complex is named *Sea Lock IJmuiden* and was opened in 2022. It has the following physical dimensions: 545 m in length, 70 m in width, and 17.75 m in depth. Sea Lock IJmuiden was built to accommodate further growth in vessel traffic and size, enabling the operation of design vessels with draughts up to 13.75 m during low tide. When in operation, the lock contributes significantly to saltwater intrusion. During normal environmental conditions, the intruded saltwater is contained by upstream freshwater discharge, and lock operation is driven by actual vessel demand. Vessels approach the lock complex when passing the 5-mile distance from the breakwaters or passing the Houtrak transect in the NSC (Fig. 2(a)). Here, the vessels' pilots announce their estimated arrival time at the lock to the lock master, who then informs the lock operator—responsible for operating the lock gates and initiating levelling, thereby communicating with the pilots—of incoming vessels so that the lock operation can be coordinated (based on personal communication with lock masters and pilots, July 2024). As there are no specific waiting areas for the lock complex, vessels wait by reducing their sailing speed; in case of longer waiting times, vessels wait in offshore anchorage areas and at the terminal.

During droughts, reduced freshwater supply in combination with continuing normal lock operation can cause salinity limits in the NSC to be exceeded (near the measurement station at Diemen, see Fig. 1), posing risks to water quality and drinking water production. This occurred in the summer of 2022, when the water management authorities imposed 12-h lock operation windows as a temporary operational countermeasure to limit the saltwater intrusion (Hendriks and Mens, 2023). Although successful in limiting the NSC's salt intrusion length, this operational countermeasure caused significant vessel delays and subsequent economic loss for water transport, clustering vessels in a reduced number of lockages. Moreover, the measure's success primarily relies on additional water supply from the Waal River and water storage of Lake Marken to combat saltwater intrusion at the NSC and supply freshwater to the west of the Netherlands via two emergency water supply systems: the Klimaatbestandige Wateraanvoervoorziening (KWA) (in English: *Climate-resilient water supply*) and Doorvoer Krimpenerwaard (DKW) (in English: *Krimpenerwaard Throughflow*). This freshwater is then unavailable for the Maasmond, where it is critically needed to combat saltwater intrusion (Fig. 1)—affecting other water intake stations and drinking water plants—and for maintaining higher water levels in the Waal River to sustain already impacted inland water transport.

2.2. Measurement campaign: Available data

This study uses the following data of Sea Lock IJmuiden, measured by Deltares between the 20th of February at 07:00 and the 20th of March at 11:00 during a campaign to evaluate nautical procedures in relation to the density-driven exchange flow of salinity: water level and salt concentration—derived from temperature and conductivity—data

Fig. 1. Overview of the study area in the Rhine–Meuse Delta. Freshwater must be allocated to combat saltwater intrusion (orange arrows) through the Maasmond and the NSC–ARC system, driven by lock operations at IJmuiden (top of the figure), while also meeting the demands of users: drinking water, water safety, agriculture, and industry. The width of the freshwater discharges (white arrows) roughly represents the distribution of river discharges during droughts. The directly affected waterboard (light area) by the lock operations is **A** Waterschap Amstel, Gooi, Vecht; indirectly affected waterboards (shaded areas) are: **B** Hoogheemraadschap De Stichtse Rijnlanden, **C** Hoogheemraadschap van Rijnland, **D** Hoogheemraadschap van Delfland, **E** Hoogheemraadschap van Schieland and the Krimpenerwaard, **F** Waterschap Rivierenland, and **G** Hoogheemraadschap Hollands Noorderkwartier.

at specific locations in and outside the lock chamber, logged lock gate-status data, and vessel dimension, lock entry and exit time data (hereafter jointly called vessel passage data) (van der Hout et al., 2024). During this campaign, a total of 375 levelling operations were performed: 171 inbound operations, of which 22 empty, and 204 outbound operations, of which 56 empty. Furthermore, we identified 222 gate-open phases at the sea and 220 at the canalside. The higher number of gate-open phases relative to levelling phases reflects the practice of the lock operator of closing the gates between successive lock operations when sufficient time is available. This occurred 47 times on the seaside (with 23 times requiring a levelling operation due to tidally varying water levels), and 44 times on the canalside (not requiring any levelling operation due to the constant water level at the canal.

Conductivity (C, denoted σ), temperature (T), and hydraulic pressure (D) were measured at four locations near both lock gates (Fig. 2), namely: 26.0 m in front of and 30.0 m behind the seaside's gate—respectively at the northern and southern wall—and 30.5 m in front of and 16.0 m behind the canalside's gate—also respectively at the northern and southern wall. At each location, five CTD-divers were placed at the following depths z: 1.5 m, 5.5 m, 9.5 m, 13.5 m and 17.0 m below NAP. From this data, water density was derived using the Equation of State of Seawater (EOS) of UNESCO (1981). A 15–second measurement sample rate was used. There are four periods with missing data, as the sensors had to be changed. During the periods of missing data, water levels from the nearby permanent monitoring location of Rijkswaterstaat are used; they matched well with the measured water levels during the campaign. Unfortunately, no measurements were available to support salt concentration estimates for these gaps.

The operational data consists of logged status data of both lock gates. In addition, pilots of the Dutch Pilot Association (in Dutch: *Loodswezen*) logged the vessel passage data, including their arrival and departure date and time at and from the lock, their dimensions (i.e., length overall, breadth and draught), and their sailing direction. Also, the number of levelling operations is monitored, including empty levelling operations. More technical details have been published in Deltares (2023).

3. Materials and methods

To evaluate the performance of the ZSF in forecasting salt intrusion fluxes in its lock cycle-average and phase-wise mode, the predictions from the method applications must be compared with the observations. For this purpose, we first introduce the ZSF in Section 3.1. Subsequently, we elaborate on the data processing of the measurement data (outlined in Section 2.2) to estimate salt intrusion fluxes per lock phase for method validation in Section 3.2. Next, we present the nautical traffic simulation library OpenTNSim and how it enables predicting time-varying gate-open durations based on vessel traffic data in Section 3.3. Last, we explain the modelling strategies for estimating saltwater intrusion fluxes with the cycle-averaged and phase-wise implementations of the ZSF and its coupled phase-wise implementation with the nautical traffic model in Section 3.4.

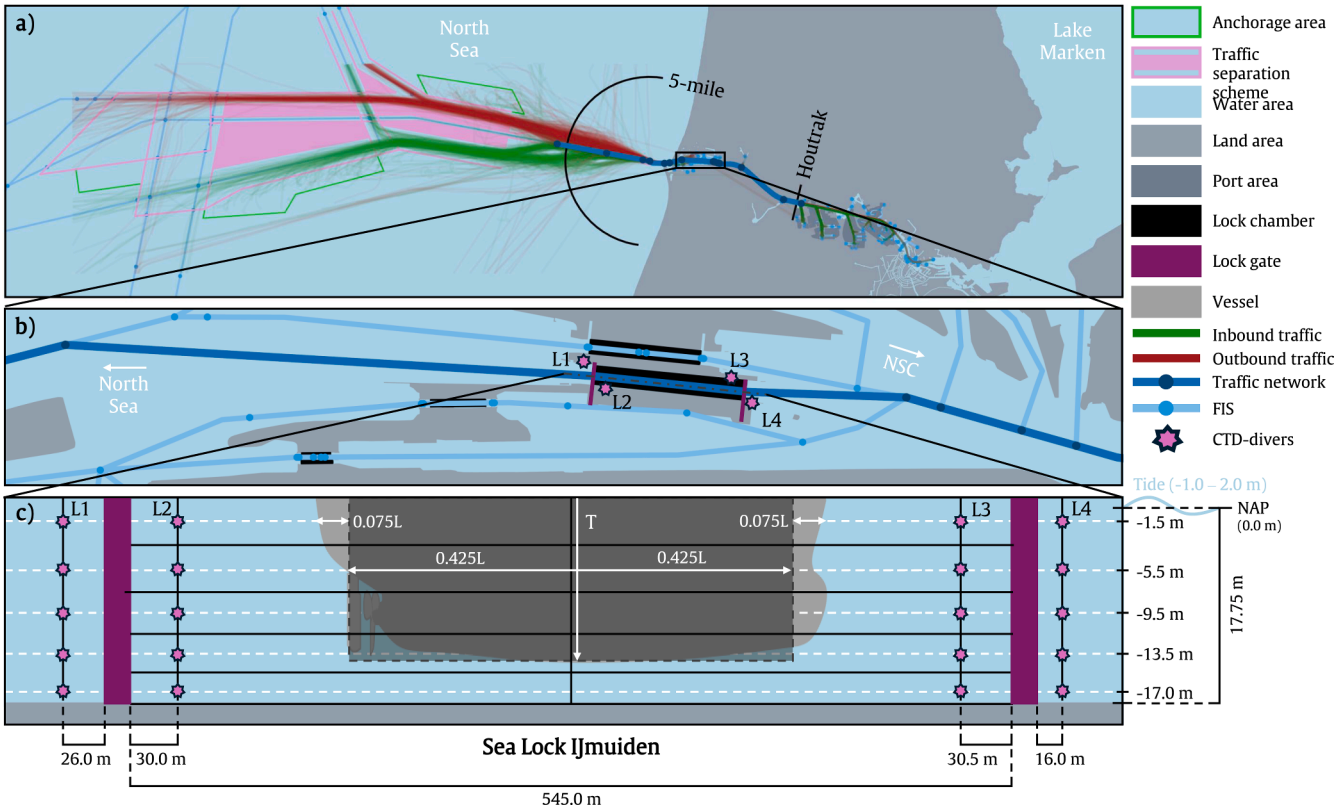

Fig. 2. Overview of the measurement campaign: **a)** the seagoing nautical traffic system between the North Sea and the Port of Amsterdam via the IJmuiden locks and the North Sea Canal, **b)** the IJmuiden lock complex and location of the measurement lines; and **c)** a longitudinal cross-section of Sea Lock IJmuiden with the location (x,z) of the divers, and the effect of a vessel occupying part of the lock chamber volume.

Table 1
An overview of the exchange flux processes in the ZSF during high water at sea: yellow arrows show inward salt fluxes and white arrows outward fluxes. The yellow arrows represent salt intrusion fluxes into the lock chamber and the canal, while white arrows represent freshwater losses.

Phase	Vessels sailing out	Levelling & density current	Vessels sailing in
Levelling to canal	*n/a*		*n/a*
Gate open at canal		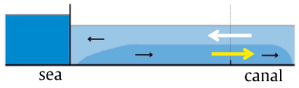	
Levelling to sea	*n/a*	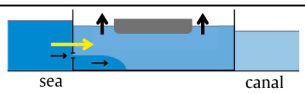	*n/a*
Gate open at sea		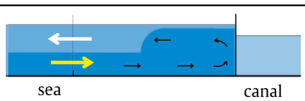	

3.1. Lock exchange model: The Zeesluisformulering

The ZSF is an analytical, semi-empirical lock exchange model, developed by Deltares (Weiler et al., 2019). It quantifies exchange fluxes between the lock chamber and the opposing harbours through water volume and salt mass balances expressed in m^3 and kg, respectively. For this, the method discretises the lock operation in four separate phases (Table 1): a levelling phase to the canal, a gate-open phase at the canal, a levelling phase to the sea, and a gate-open phase at the sea. This subsection discusses the fundamentals of the ZSF; we refer to Weiler et al. (2019) for more details on the method.

Exchange of water per phase occurs in the model through the following processes (Table 1): (1) the levelling flux, (2) the influence of vessels sailing into and out of the lock, and (3) density-driven exchange flux. The exchange fluxes are assumed to occur as sequential, independent events—following an event-based modelling approach—while in reality fluxes (2) and (3) occur simultaneously. Moreover, the salt concentration in kgm^{-3} is assumed to be uniformly distributed over the entire lock chamber, and uniform at the opposing harbours (Weiler et al., 2026); vertical stratification is neglected. Levelling is gravity-driven and leads to a water volume flux that depends on the horizontal lock dimensions and the locking head, defined as the difference in water level between

the lock chamber and the harbour to which the chamber is levelled. Water flows into the chamber when the lock is levelled towards a higher water level, and out of the chamber when levelled towards a lower water level. This leads to saltwater intrusion when the water level at sea is higher than in the canal, and, vice versa, to freshwater losses. Note that Table 1 only shows the situation during high water at sea; the low water situation leads to a reverse direction for the salt transport during levelling.

During the gate-open phases, the following exchange volumes of water are accounted for in the ZSF (Table 1): (a) vessels sailing out of the lock, (b) density-driven currents; and (c) vessels sailing into the lock. At the start of the gate-open phase, the total water volume associated with departing vessels from the previous lock operation is assumed to enter the lock chamber instantaneously, immediately before the start of the density-driven current. This current is initiated when the lock gate is halfway opened and stops when the gate is halfway closed. Similarly, the total water volume corresponding to arriving vessels of the next lock operation is instantaneously removed at the stop of the density-driven current—the end of the gate-open phase. At the canalside, vessels sailing out of the lock lead to freshwater losses and vessels sailing into the lock to saltwater intrusion; the opposite applies at the seaside.

During the density-driven current—generally the most dominant exchange mechanism—the water in the lock chamber is gradually replaced by water of the harbour, such that inflow and outflow fluxes occur simultaneously (Table 1). The water volume exchanged due to the density-driven current, V_{exchange}, without a bubble screen is estimated semi-empirically according to Eq. (1), as proposed by van der Burgh and de Vos (1962):

$$V_{\text{exchange}} = V_{\text{L}} \tanh\left(\frac{t_{\text{open}}}{t_{\text{LE}}}\right) \tag{1}$$

where V_{L} is the volume of water in the lock chamber during the gate-open phase [m^3], t_{open} is the gate-open duration [s], and t_{LE} is the theoretical lock exchange time [s], defined as the time it takes for the density-driven current's front to travel the full length of the lock chamber and back, reflecting against the closed gate. For a lock without a sill and flushing, this theoretical lock exchange time t_{LE} is estimated in the ZSF according to Eq. (2), as established by Abraham et al. (1973):

$$t_{\text{LE}} = \frac{2\,L_{\text{L}}}{c_i} = \frac{2\,L_{\text{L}}}{\frac{1}{2}\sqrt{\frac{gH\Delta\rho}{\overline{\rho}}}} \tag{2}$$

where L_{L} is defined as the length of the lock chamber [m], and c_i the initial speed of the density front [ms^{-1}], which depends on g the gravitational acceleration in [ms^{-2}], the water depth H of the lock [m], the difference in water density between the lock chamber and the harbour $\Delta\rho$ [kgm^{-3}], and $\overline{\rho}$ the mean water density between both opposing harbours [kgm^{-3}]. Note that the hyperbolic tangent in Eq. (1) ranges from 0 to values asymptotically approaching 1 for positive arguments. According to this, 76.1% of lock volume is exchanged when the gate-open duration equals the theoretical lock exchange time.

The magnitudes of all exchange fluxes are computed by multiplying the exchanged water volume by the average salt concentration of the water from which the flux is directed, either the harbour or the lock chamber. Hence, the lock chamber's salt concentration increases when more saline water flows in, and conversely decreases when less saline water enters the lock chamber. The salt concentration remains unchanged when water flows out of the lock chamber. The net effect of the density-driven exchange current fluxes is to increase salinity in the lock chamber at the seaside (salt loading) and decrease it at the canalside (salt intrusion).

The input of the ZSF comprises static geometrical, hydrodynamic, lock operation, and vessel parameters. Geometrical parameters consist of the dimensions of the lock chamber (i.e., length, width and depth, and, if applicable, sill heights), and the depth of the opposing harbours. The hydrodynamic input parameters entail water levels and uniform salt concentrations at both sides of the lock and the lock chamber. When the ZSF is applied, each phase continues with the previously estimated water level and salt concentration for the lock chamber. Lock operation parameters comprise the gate-open and levelling phase durations. Vessel parameters consist of the total volume of water that vessels occupy in the lock chamber for both inbound and outbound lock operations. Depending on the specific mode of the ZSF (i.e., either cycle-averaged or phase-wise, see next paragraph), the above data should be specified as lock cycle-steady values or for each lock operation phase individually.

The ZSF can be applied in two different modes: a lock cycle-averaged and a phase-wise mode. In the lock cycle-averaged mode, lock cycles are run with periodically fixed, operation-averaged input parameters. These include periodically constant lock cycle frequencies, constant gate-open and levelling phases durations, constant water levels and salt concentrations at the opposing harbours, and constant inbound and outbound vessel volumes. In this mode, the method iteratively determines an equilibrium salt concentration in the lock chamber for each operational phase of the lock operation, based on which the mass fluxes to both harbours can be calculated. The fluxes of water and salt of the separate phases of the lock cycle are added up and divided by the duration of the lock cycle to determine the cycle-averaged fluxes of water and salt through both lock gates. The mode is frequently used in practice, as time series or estimates for varying gate-open durations are often lacking.

In the real world, however, the input parameters would vary per lock operation caused by the dynamic arrival process of vessels and the varying water levels and salt concentrations at the harbours. This leads to phases with different durations and water exchange flux magnitudes. Generally, a series of sequentially varying short and long gate-open durations results in less saltwater intrusion compared to a constant gate-open duration. To account for this, the ZSF can be run in the phase-wise mode, with each phase run with specific input parameters. For gate-open phases, this involves variable inbound and outbound vessel volumes, gate-open durations, water depths, and salt concentrations. For levelling phases, this involves variable heads, levelling durations, and salt concentrations.

To account for the variability in gate-open durations in lock cycle-averaged mode, representative values at both sides of the lock can be calculated using two calibration factors. First, a calibration factor, called c_{DOT}, converts the operation-averaged gate-open duration to a representative gate-open duration that yields an operation-averaged saltwater intrusion flux for the density-driven current. It accounts for the non-linear relationship between gate-open duration and salt intrusion mass (Eq. (1)). c_{DOT} is site-specific, depending on the lock operation. Note that the factor does not modify the lock operation frequency; the average gate-open duration is still used to simulate the lock operation times. Second, there is a factor that corrects for an asymmetry of the gate-open duration between the sea and the canalside.

To date, no formula exists that can provide a reliable value for the calibration factor prior to the simulation. It requires either cross-model calibration: a phase-wise simulation requiring phase-varying gate-open durations. Furthermore, there are no calibration factors in the phase-wise mode. Both application modes are fast and have similar computational costs, making the less detailed input parameters the only benefit of using a lock cycle-averaged over the phase-wise application.

3.2. Measurement data processing

To compare the performance of the lock cycle-averaged and phase-wise modes of the ZSF, both periodically cycle-averaged and phase-varying input parameters must be provided. Furthermore, to validate the predictions of the ZSF, we must estimate the saltwater intrusion mass fluxes for each lock operation phase based on our observations. For this, we designed a workflow that combines the hydrodynamic and geospatial data, and logged vessel passages and gate operations from the measurement campaign (Fig. 3). The derivation of the model's input parameters and validation data from this dataset requires the following

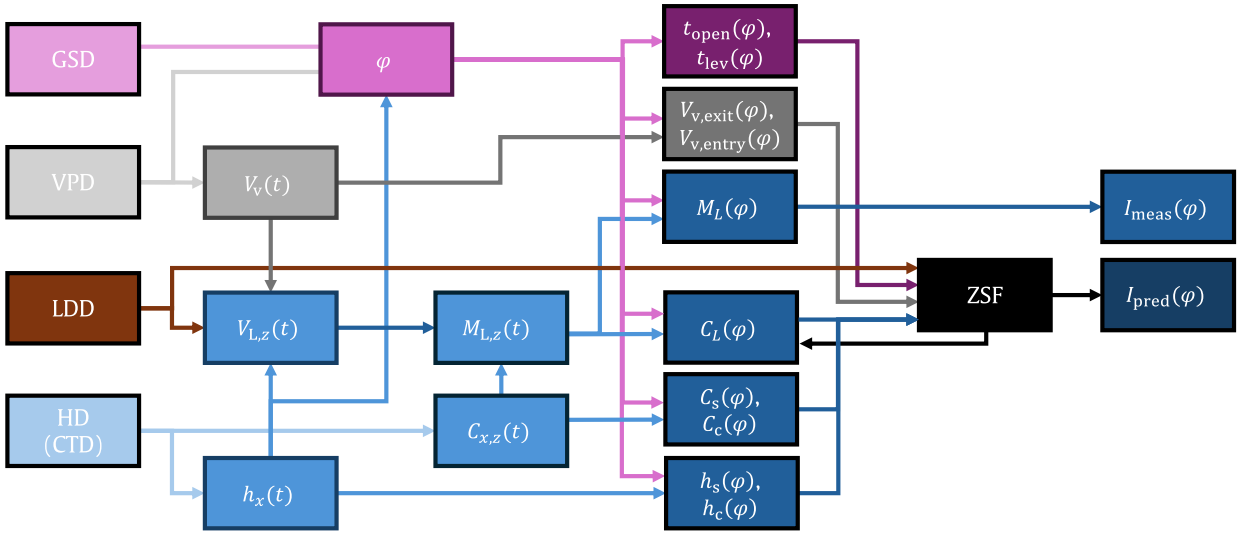

Fig. 3. Workflow of predicting saltwater intrusion with measurement data and the ZSF. The abbreviations and symbols are explained in the text.

steps: (1) identifying the lock operation phases, (2) coupling the hydrodynamic and nautical boundary conditions, and (3) calculating the saltwater intrusion mass fluxes.

The first step is to identify the lock operation phases. The gate-open and levelling phases are distinguished using the Gate Status Data and Hydrodynamic Data (respectively GSD and HD in Fig. 3), shown in Fig. 4(a). For each phase φ, the following information is derived: the total durations of the gate-open or levelling phase, $t_{open}(\varphi)$ and $t_{lev}(\varphi)$, the volumes of exiting and entering vessels, $V_{v,exit}(\varphi)$ and $V_{v,entry}(\varphi)$, the lock chamber's (denoted as L) total salt mass $M_L(\varphi)$ and salt concentration $C_L(\varphi)$; and, at the sea and canal (denoted as s and c, respectively), the salt concentrations, $C_s(\varphi)$ and $C_c(\varphi)$, and water levels, $h_s(\varphi)$ and $h_c(\varphi)$.

Following the definitions of the ZSF, we determine the start and end times of the gate-open phases as the time when the gate is half opened and half closed, respectively, using the GSD data. This results in the phase-varying gate-open durations, $t_{\text{open}}(\varphi)$. The direction of the phase corresponds with the side to which the gate opens: to the canal (inbound) or to sea (outbound). Based on these phases, successive gate-open phases on the same side were identified. Here, the lock gate on a given side closes and subsequently reopens before the next operation on the opposite side; these we treated as individual gate-open phases (e.g., between 8:15 and 9:05, and 10:40 and 12:40 in Fig. 4). The start and stop times of the levelling phases were determined from the water level. For this, the hydraulic pressure (D) at each location x over time, t, is converted into water levels, $h_x(t)$ [m], by subtracting the depth at which the diver is located and correcting for the ambient air pressure (Fig. 4(b)).

The duration of levelling per phase, $t_{\text{lev}}(\varphi)$, is defined as the longest continuous period during which the rate of water level change is above a threshold of 0.1 cm/s while both lock gates are closed. For this, we use the 2.5-min rolling average of the locking head difference. This threshold was determined by visual analysis of the water level data. Note that successive gate-open phases at sea may also require a levelling operation, as there is a tidal water level variation(e.g, at 09:00 h in Fig. 4). In case there is no water level difference between two gate-open phases on the same side, the levelling phase is assumed to occur instantly.

Given the exact start and stop times of the phases, the total occupied water volumes by exiting and entering vessels per phase can now be determined using the Vessel Passage Data (VPD in Fig. 3). These volumes are calculated by the sum of each vessel's product of their length, beam, draught, and a block coefficient of 0.85, which is typical for tankers and dry bulk vessels (Ha and Gourlay, 2017), being the main vessel types at IJmuiden. Here, it is assumed that all vessels have a perfectly squared frontal cross-section and are located in the centre of the lock (Fig. 2(c)). Combined with the Lock Dimension Data (LDD in Fig. 3) and determined time-varying water levels, the water volumes in the lock chamber can be determined over time t and per depth layer z: $V_{\text{L},z}(t)$. Here, we use the width-averaged nearest-neighbour volume associated with each diver, visualised in Fig. 2(c) by the black-lined grid-cell boundaries. The resulting water volumes for each diver are corrected for the volume occupied by vessels in the lock for each depth layer over time. Missing horizontal vessel dimensions were taken as the fleet's average values. Missing vessel draughts were estimated using a fitted power law, following the average relation between the vessels' surface areas and draughts. Within the measurement campaign, a maximum of four seagoing cargo vessels per lockage were levelled, occupying a maximum of merely 26.7% of the total volume of the lock chamber (Fig. 4(c)); 59 empty lock operations were performed.

The salt concentrations per phase at each location x and diver z, $C_{x,z}(t)$, expressed in kgm^{-3}, can be derived from the measured conductivities and temperatures, according to Eq. (3):

$$C = \frac{S(\sigma, T)}{1000} \cdot \rho(S, T) \tag{3}$$

where S is salinity [PSU], resulting from the measured conductivity σ [mScm^{-1}] and temperature T [C°] of the water, based on Deltares (2023), and ρ [kgm^{-3}] the corresponding density given the salinity S [PSU] and temperature T [C°] of the water, based on the UNESCO (1981) formulation. The factor 1000 is used to convert the salinity in [PSU], equivalent to [gkg^{-1}], to a dimensionless parameter in [kgkg^{-1}]. This conversion step is an addition compared to earlier applications of the ZSF, which assume that salinity and salt concentration are equivalent (Weiler et al., 2026). We found that this step leads to slightly improved model performance in our case study. In line with the ZSF, we use uniform, depth-averaged salt concentrations. The salt concentrations at the sea and the canal, each measured by one line of CTD-divers, were determined through depth-averaging, leading to the raw salt concentrations, indicated with the light-coloured lines for the sea and canalside in Fig. 4(d). We decided to disregard salt concentrations in a harbour when, during gate-open and levelling phases, water is entering this harbour, including 15 min after these events. The density-driven current significantly changes the measured harbour salt concentrations due to their proximity to the lock chamber (e.g., around 02:30 h for the salt concentration in the canal, and 05:45 h at sea in Fig. 4(d)). Then, the concentrations are temporarily unrepresentative of the undisturbed situation of these harbours, which should be used as the boundary condition for the ZSF. The gaps were filled through linear interpolation. In

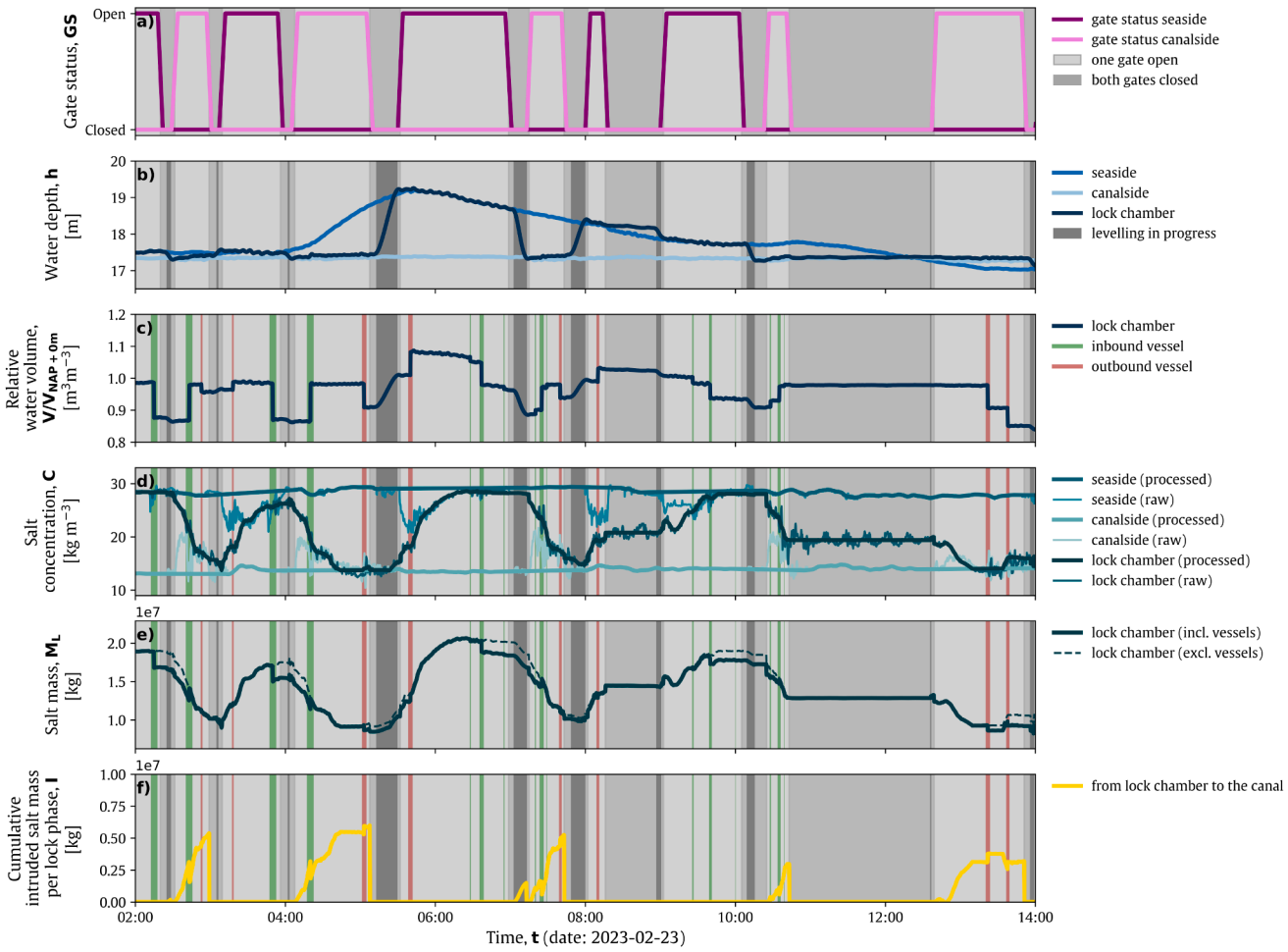

Fig. 4. Processing of the measurement data: **a)** the lock's gates statuses and vessel passages to determine gate-open phases and vessel volumes, **b)** the water levels around and inside the lock chamber to determine levelling operations and lock chamber volumes, **c)** the water volume of the lock chamber relative to water volume when the water level in the lock is at 0 m + NAP (Fig. 2(c)) and arrival and departures of inbound and outbound vessels (thicker lines indicate bigger vessels), **d)** the calculated average salt concentration in the lock chamber, and both opposing harbours, **e)** the calculated total salt mass inside the lock chamber; and **f)** the calculated cumulative salt intrusion into the canal per lock phase.

addition, a 5-min moving average was applied to smooth sudden peaks, leading to the processed salt concentration, indicated with the wider and darker-coloured lines for the sea and canalside (Fig. 4(d)).

For the lock chamber, we calculated the phase-varying salt concentrations differently, as there are two lines of CTD-divers and vessels within the water volume (Fig. 2(c)). First, the divers' raw salt concentration measurements are averaged for each depth layer z, and the resulting values are multiplied by the water volumes of each depth layer $V_{\mathrm{L},z}$. Multiplying these volumes by the salt concentrations results in the time-dependent salt masses per depth layer in the lock, $M_{\mathrm{L},z}(t)$. From this, the time-varying raw total salt mass in the lock chamber, $M_{\mathrm{L}}(t)$, can be determined (Fig. 4(e)), and subsequently the raw time-varying lock chamber-averaged salt concentration, $C_{\mathrm{L}}(t)$, by dividing $M_{\mathrm{L}}(t)$ by the sum of $V_{\mathrm{L},z}(t)$ (Fig. 4(d)). The raw salt concentrations during idle times of the lock—when there is no exchange of water—artificially vary. These variations emerge from the combined effect of standing internal waves and the limited spatial resolution of measurement locations in the lock chamber (e.g., between 08:15 and 09:00, and 10:45 and 12:45 h in Fig. 4). We therefore processed the concentration (indicated with the darker-coloured line for the lock chamber in Fig. 4(d)) by taking the mean over these idle periods. For the non-idle times of the lock, separate 5-min moving averages were applied to smooth sudden peaks. In addition, observed salt concentrations above or below the seaside and canalside concentrations were adjusted to match the seaside and canalside concentrations (e.g., at 05:00 and 13:30 h in Fig. 4).

As a last step, the measured saltwater intrusion mass for each phase, $I_{\mathrm{meas}}(\varphi)$, has to be determined for validation purposes. For this, the difference of the total salt mass in the lock chamber at the start and stop of each phase had to be determined: $M_{\mathrm{L}}(\varphi)$. Salt intrusion occurs when there is a positive flux during gate-open phases at the canalside and during levelling phases towards the canalside when the water level at sea is higher (Fig. 4(f)). The predicted saltwater intrusion masses, $I_{\mathrm{pred}}(\varphi)$, follow from the ZSF (Fig. 3).

3.3. Nautical traffic model: OpenTNSim

As an additional step in this paper, we employ a nautical lock passage model that can predict realistic gate-open and levelling durations, and total volumes of exiting and entering vessels per lock operation phase, based on vessel traffic, lock dimensions, and water level data. This reduces the fully data-driven workflow (Fig. 3) to a more simulation-based workflow, presented in Fig. 5, and reduces the dependency on gate-status data to apply the ZSF in a phase-wise mode.

The nautical lock passage model is built within the OpenTNSim library, which was initiated and is under development by the Delft University of Technology (van Koningsveld and den Uijl, 2019; Baart et al.,

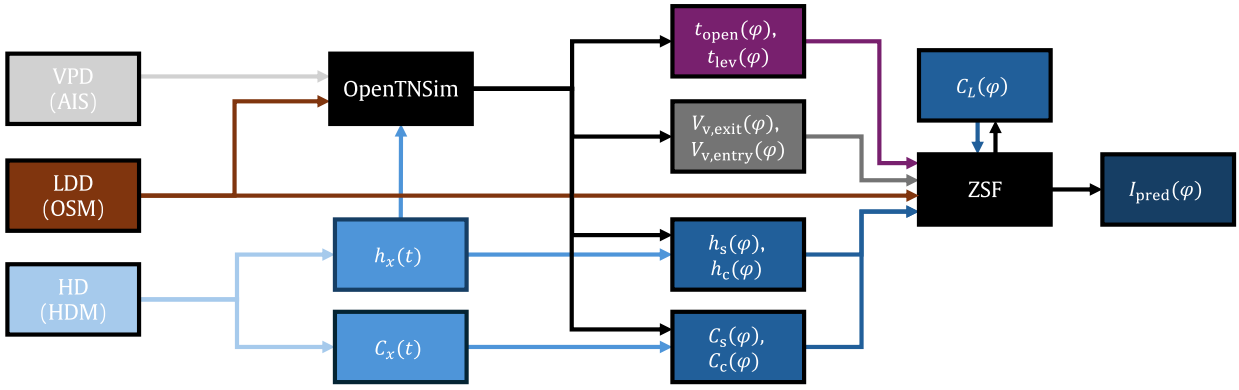

Fig. 5. Workflow of predicting saltwater intrusion with OpenTNSim predicting phase information for the ZSF without using gate status data.

2022; Bakker et al., 2024, in prep.). This Python-based library enables discrete-event simulation modelling of vessel agents navigating over a water transport network—represented as a graph of nodes and edges—while jointly interacting with port and waterway infrastructure, and the physical environment (e.g., water levels and current velocities). Within the library, a separate "Lock"-module exists that enables the allocation of "LockComplex"-objects in the waterway graph. The object consists, at least, of a one-dimensional lock chamber and two waiting area objects, at user-defined distances from the lock, but can include more lock chambers and waiting areas. It includes a "LockMaster", resembling the lock complex's control centre, which registers arriving vessels (i.e., when they arrive at a specific registration node). This entity assigns the vessels to the lock operation planning (i.e., a location in the lock chamber for a specific lock operation), guiding them towards and from the lock, and instructs vessels to wait if needed. A "LockOperator" operates the gates and levelling valves of a lock chamber. The method's output comprises the vessel behaviour around the lock complex, including vessel delays, and the lock operation behaviour, namely the initiation and stop times of levelling and gate movements (i.e., opening and closing). Using these outputs, lock operation phase-specific information can be derived, consisting of levelling and gate-open durations, as well as the total vessel volumes for each specific lock operation. This phase-specific information is directly used as input for the phase-wise application of the ZSF, added with hydrodynamic data (i.e., water levels and salt concentrations, Fig. 5).

OpenTNSim requires the following input at minimum: (1) geospatial data, entailing the dimensions and layout of the lock complex and the network of waterways, (2) vessel data, namely the vessels' arrival times, dimensions and sailing speeds over the network; and (3) lock operation data, such as the duration of moving the gate, as well as the levelling duration. Optionally, (4) hydrodynamic data, comprising water levels at the harbours, can be added to determine locking head-dependent levelling durations. Moreover, operational hours of the lock complex can be defined, as well as vessel speeds for sailing into the lock, sailing out of the lock, and the manoeuvring speeds within the lock chamber. In addition, the method can imitate specific lock operation strategies, for example, that limit saltwater intrusion, such as gate closing between subsequent vessel departures and arrivals at the same side, convoy formation to reduce the total sailing-in duration, and vessel clustering. For this, the following deterministic lock operation parameters can be used as input to the nautical traffic model:

1. the time gap between the start of the gate-opening in advance of the arrival of the first vessel (in case both gates were closed in between operations or an empty lockage was required),
2. the time between the last departuring vessel from the previous lockage and the first arriving vessel from the next lockage (expressed in distance to the lock chamber where these vessels encounter each other),
3. the time gap between two successive vessel arrivals in the same lock operation,
4. the levelling duration (can also be included as a function of the water level difference between the harbours),
5. the time gap between two successive vessel departures of the same lock operation,
6. the time gap between gate-closure after the last vessel departure (in case both gates can be closed in between operations or an empty lockage is required); and
7. clustering time (i.e., the maximum allowable waiting time of a vessel after mooring in the lock chamber for other vessels to arrive to join the lock operation; the vessel will not be instructed to wait if no vessels are expected to arrive within this time).

Herein, the gate-open durations are affected by parameters 1–3, and 5–7, while the lock operation duration and subsequent vessel delays are dependent on the efficiency of the lock operation, namely parameters 2–5 and 7.

To apply the nautical traffic model to the presented case study (Section 2), the Rijkswaterstaat's Fairway Information System (FIS)-graph is used as the network of fairways. From this network, a subgraph was created, spanning the waterways in between the lock registration nodes (i.e., the 5-mile node to the Houtrak-node), to which the "LockComplex"-object was added (Fig. 2(a)). At the edge that encompasses the lock chamber of Sea Lock IJmuiden, a lock chamber was added with dimensions taken from publicly available data of Rijkswaterstaat (Fig. 2(b)). Vessels were generated according to their logged arrival times at the lock, dimensions, and directions. To obtain these arrival times at the network boundaries (i.e., the registration nodes), the arrival times at the lock were substracted with the average sailing time from the registration nodes to the lock. For this, we used Automatic Identification System (AIS) data consisting of messages with the location and speed of the vessels. Here, we created vessel trajectories, which we mapped and aggregated to derive average sailing speeds on the network. Water levels were derived from the measurement data (Section 3.2).

To imitate the locking strategy at IJmuiden—with the goal of obtaining realistic gate-open durations per lock operation phase (to serve as input for the ZSF)—values for the above lock operation parameters in OpenTNSim had to be derived (Fig. 6). In this study, we derived these based on combining the gate status, water level, vessel entry and exit time (from the vessel passage data), and vessel trajectory data (from the AIS data); however, as shown later in this paper, comparable results could have been obtained using best-guess values. From this dataset, we observe a wide distribution in gate-open durations, caused by the dynamic pattern of arrival of vessels and the variable lock operation behaviour of lock operators and among them in certain situations. In 33.9% of the gate-open phases, the open lock gate had been directly closed between the exit of the vessels. Here, the lock operator generally re-opens a gate 30 min before the arrival of the first vessel of the next lock op-

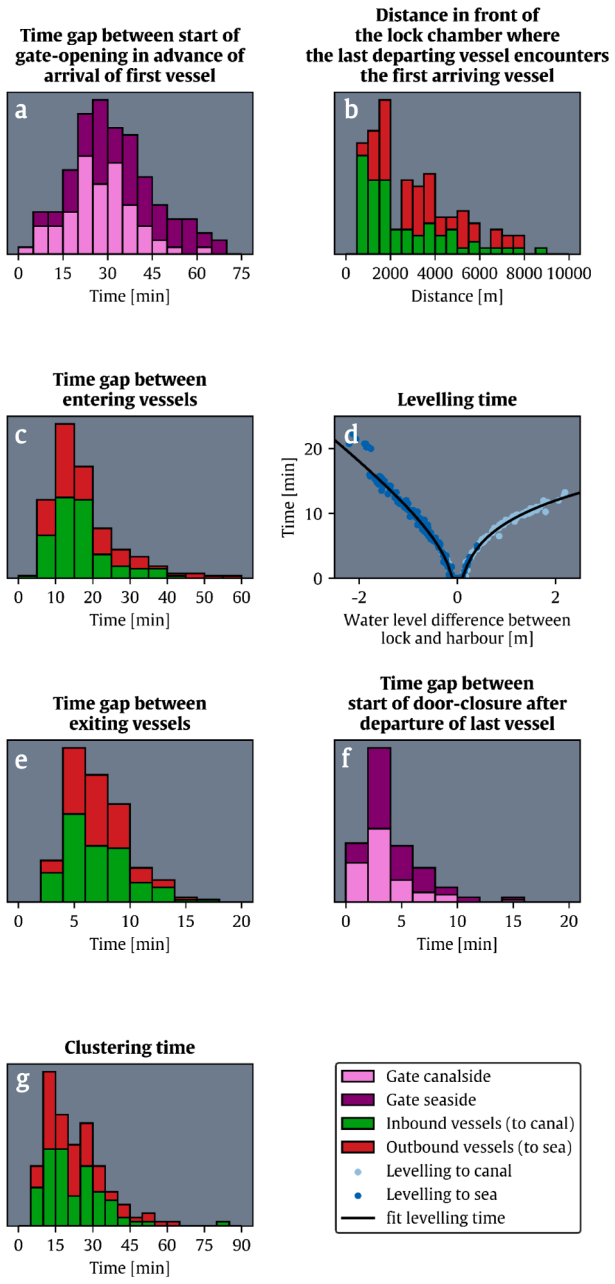

Fig. 6. The distributions of the lock operation parameters used in the nautical traffic model.

eration (Fig. 6(a)). In the rest of the lock operations, the exit of vessels is directly followed by the entry of vessels within the same gate-open duration, generally lasting up to an hour, but longer durations are not uncommon. Based on the vessel trajectories for these operations, exiting and entering vessels can safely encounter each other at a minimum distance of approximately 1000 meters from the lock gate (Fig. 6(b)). Entering vessels typically sail in after 15 min of each other (Fig. 6(c)); no gate closures were observed in between vessel arrivals of the same lock operation. Given Fig. 6(d), observed levelling times are fully dependent on the locking head, following a curve that is interestingly different for levelling towards the canal and sea. Exiting vessels follow each other faster, with a modal time of 5 min (Fig. 6(e)). If the lock operator decides to close the door after the last vessel has left the lock chamber, this typically occurs within 5 min (Fig. 6(f)). The clustering time is set to a (visual) maximum of 60 min of the first vessel (Fig. 6(g)).

3.4. Modelling strategy

To assess the predictive power of the ZSF in the estimation of salt intrusion, we first benchmark the method by validating it for each phase separately, comparing the observed and modelled salt mass fluxes using Pearson correlation analysis. In continuation, we compare the performance of the ZSF in the following model application modes: (1) lock cycle-averaged with steady hydrodynamic conditions, (2) lock cycle-averaged with periodically varying hydrodynamic conditions, (3) phase-wise with observed gate-open durations; and (4) phase-wise with gate-open durations assimilated using OpenTNSim. Here, in contrast with the validation run, the exchange fluxes for the next phase are calculated with the predicted salt concentration for the lock chamber at the completion time of the previous phase. Furthermore, for the lock cycle-average runs, we distinguish between fully constant hydrodynamic boundary conditions and time-varying conditions by calculating new equilibrium situations for each lock operation cycle separately. Here, we do not apply site-specific calibration prior to the simulation, reflecting the conditions of a future scenario. The comparison between the model runs is performed by quantifying the error in total salt intrusion mass. Thereby, we excluded the phases during periods of missing data from the validation.

4. Results

The results are structured as follows: validation of the ZSF for individual lock operation phases (Section 4.1), modelled gate-open duration with OpenTNSim (Section 4.2); and application of the ZSF to estimate long-term cumulative saltwater intrusion mass fluxes (Section 4.3).

4.1. Validation: Observed phase-wise salt exchange

Based on the observed change in salt mass per lock operation phase, $1.28 \cdot 10^9$ kg of salt intruded into the canal during the measurement campaign. This corresponds to a time-average salt load of 530.6 kgs^{-1}. We observe a time-averaged incoming discharge of 45.1 m^3s^{-1} of saltier water with, on average, a 11.8 kgm^{-3} higher salt concentration than canal (14.9 kgm^{-3}). Of this salt intrusion discharge flux, 42.9 m^3s^{-1} is caused during the density-driven current, and compensated by an equal outward-directed discharge of fresher water into the lock chamber. Hence, there is a net inward-directed discharge of 2.2 m^3s^{-1}, of which 1.5 m^3s^{-1} is caused by levelling, as the water levels at sea are on average slightly higher than in the canal. This levelling flux is observed to have an average salt concentration of 32.9 kgm^{-3}. Note that this concentration is higher than the depth-averaged salt concentration at sea (28.4 kgm^{-3}) due to stratification. The remaining 0.7 m^3s^{-1} of the net discharge is caused by vessel movements, as the total occupied water volume by the outbound vessels is greater than the volume by the inbound vessels. To flush out the intruded salt flux, we can estimate that a net seaward-directed freshwater discharge of 35.6 m^3s^{-1} is required, given the depth-average salt concentration at the canalside of 14.9 kgm^{-3}.

An estimated 90.6% of this flux occurs during the gate-open phase; 80.6% of the flux is caused by the density-driven current and 10.0% by outbound vessels sailing into the lock at the canalside. Despite this contribution of outbound vessels to saltwater intrusion, inbound vessels are found to limit salt intrusion by 5.3%, as they occupy water volume in the lock chamber, thereby limiting the total mass of salt that can intrude per gate-open phase. The remaining 9.4% of the salt intrusion flux can be attributed to the levelling operations towards the canal when the water level at sea is higher than at the canal.

Comparing the observed and ZSF-predicted salt exchange fluxes for each separate phase reveals that the ZSF has strong predictive power (Fig. 7). The modelling results show the best agreement with the observations of the gate-open phases: the predictive power of the intruded salt

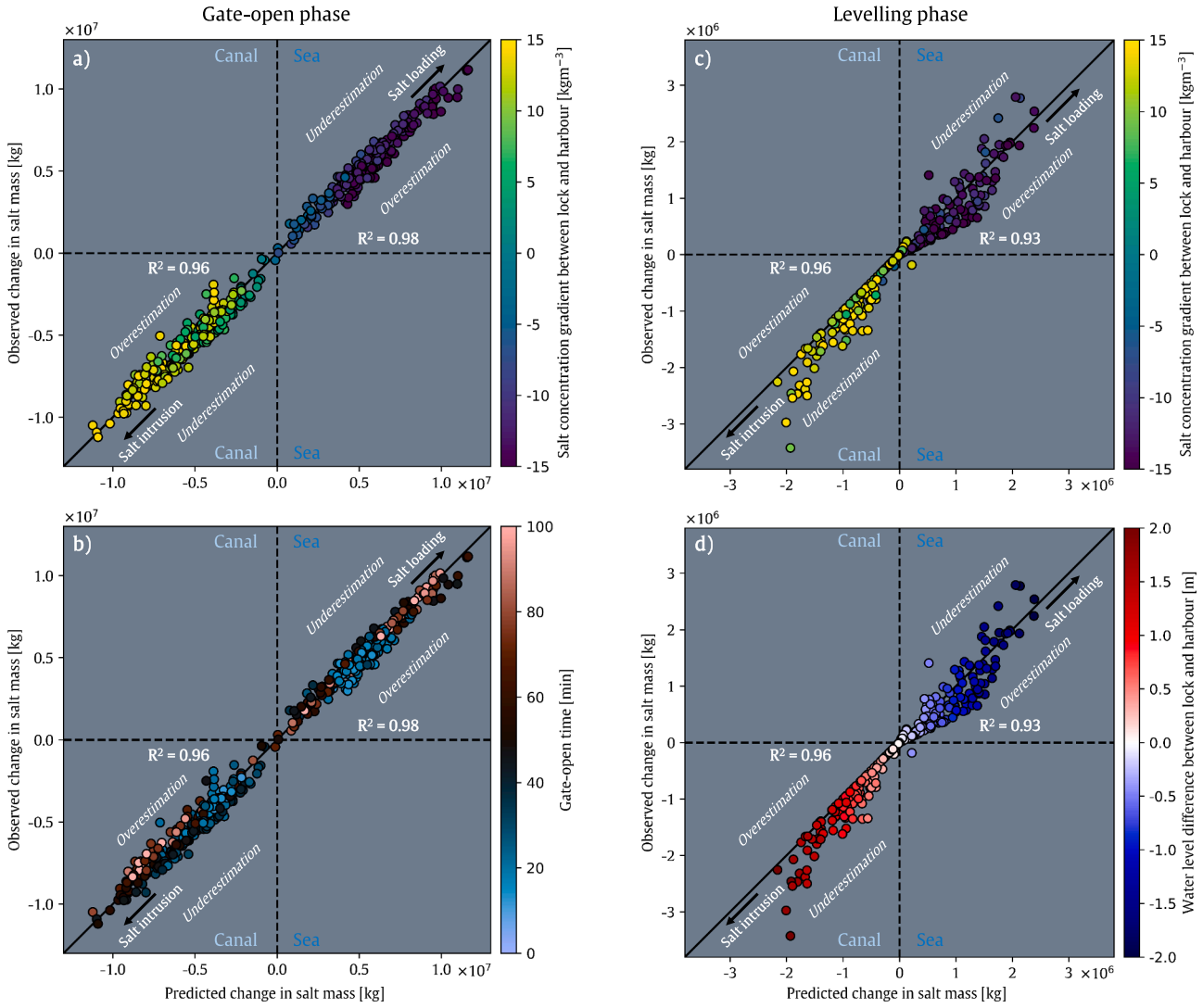

Fig. 7. Validation of the salt mass exchange during the lock phases: (1) gate-open phases as a function of **a)** the salt concentration difference between the lock chamber and the harbour, and **b)** the gate-open duration; and (2) levelling phases as a function of **c)** the salt concentration difference between the lock and the harbour, and **d)** the water level difference between the lock and the harbour. Note the different order of magnitude in salt mass exchange between the gate-open and levelling phases.

mass during the gate-open phase at the canal yields a coefficient of determination R^2 of 0.96, increasing to 0.98 at the seaside. The data matches the expectations; total salt exchange increases with increased salt concentration difference between the lock and the harbour and increased gate-open duration (Fig. 7(a)). Relative errors in the estimated salt intrusion mass per individual gate-open phase at the canalside range between −17.2% and +15.2% with respect to the observations, but absolute errors are below 5.0% in 51.7% of the events. These errors were observed to be affected by the gate-open durations (Fig. 7(b)) and correlate to a lesser extent with the salt concentration difference between the lock chamber and the canal. Short events (≤ 20 min) result in small overestimations, i.e., both the observations and model predict small exchange volumes. Intermediate events (> 20 min and ≤ 60 min) cause underestimations with a peak at 35 min, although some significant overestimations occur. This hints at a general underestimation of the speed of the density-driven current. In contrast, longer events (> 60 min) generally result in small overestimations, i.e., full lock exchanges are predicted. At the seaside, the errors are relatively smaller; relative errors range between −6.1% and +10.4%, with absolute errors below 5.0% in 86.4% of the events. The errors are largest for short-to-intermediate events (≤ 60 min) with significant overestimations, gradually decreasing with longer gate-open durations. Compared to the canalside, a similar peak of underestimations at around 35 min can be observed, but is less present due to fewer events with gate-open duration between 20 and 60 min. The errors also correlate with the salt concentration difference between the seaside harbour and the lock chamber. Underestimations are generally associated with smaller differences, with overestimations generally occurring with greater differences. Additionally, the errors are observed to moderately decrease with increasing lock chamber water volume occupied by inbound vessels.

The levelling towards the canal also shows good agreement with the observations, with an R^2-score of 0.96, which decreases to 0.93 towards the sea (Fig. 7(c) and (d)). We observe, however, a greater bias compared to the saltwater intrusion fluxes during gate-open phases, with larger errors being associated with larger exchange fluxes. For levelling towards the canal, relative errors range from −9.4% up to +0.5% with respect to the observations. Hence, an overall underestimation occurs, which is strongly correlated with the locking head with the canal, and to a lesser extent with the difference in salt concentration. The absolute errors are below 5.0% in 98.8% of the events that lead to saltwater intrusion into the canal. For levelling towards the sea, the maximum relative errors are greater, between −9.3% and +7.1%, but generally overestima-

tions. Here, absolute errors are below 5.0% in 92.8% of the events and increase with larger water heads.

Cumulatively, the ZSF predicts $1.23 \cdot 10^9$ kg of salt intrusion in the canal, where 91.9% is caused during the gate-open phase; 82.6% of the mass flux is caused by the density-driven current, 9.3% by outbound vessel sailing into the chamber, and 8.1% by levelling. This corresponds well with the observations, but there is a slight underestimation of the total salt intrusion mass of −3.7%. We found 55.9% of this error to be caused during the gate-open phases; the remaining 44.1% is associated with the levelling phases, despite the order-of-magnitude smaller flux magnitudes compared to the gate-open phases (Fig. 7). Although there are large absolute errors at some gate-open phases, the combination of under- and overestimations during this phase tends to balance out, leading to a very acceptable model performance regarding saltwater intrusion into the canal. In contrast, the levelling phases show a consistent underestimation of this flux.

During the gate-open phase at the canalside, there is a minor −2.3% underestimation of the total predicted salt exchange, compared to a minor +2.0% overestimation of this flux during the gate-open phase at the seaside. The underestimation in cumulative salt intrusion during the gate-open phase at the canal is expected to be mainly caused by the underestimation of the speed of the density-driven current. The underestimation seems, however, to be partly compensated by the neglect of stratification in the ZSF and the limited resolution of the measurements and subsequent calculation errors of the saltwater intrusion masses (Section 5.1); there is an average buoyancy or Brunt–Väisälä frequency at the lock of 0.08 s^{-1}, ranging in between the average values for the sea (0.06 s^{-1}) and canal (0.1 s^{-1}). For example, for shorter gate-open durations, we observe that the exchange current does not reach the line of CTD-divers at the closed gate, due to which we measure a smaller salt concentration difference in the lock chamber, and a subsequent overestimation of the observed salt mass exchange flux by the ZSF (Fig. 7(b)). In addition, for longer gate-open durations, we observe overestimations of the salt exchange mass flux by ZSF, as the observed lock chamber-averaged salt concentration at the end of the gate-open phases stays generally higher than the modelled concentration. This can also be attributed to a combination of limited depth measurement resolution and strong stratification. Given this stratification and the mean draught of vessels of 7.8 m, we also expect the return flow of the vessels to be fresher compared with the ZSF, which assumes the lock chamber and harbours to have a uniformly distributed salt concentration.

There is, furthermore, a cumulative structural −17.7% underestimation in salt intrusion when levelling to the canal, accompanied by a +15.5% overestimation when levelling to sea (Fig. 7(c)). For levelling to the canal, the cause of this error is expected to mainly lie in the neglect of the ZSF of stratification, rather than the limited measurement resolution. As the discharge valve is located at a depth of NAP−10.25 m, where in 63.3% of the levelling events towards the canal the salt concentration is observed to be higher than the mean concentration, more saline water is expected to intrude into the canal than as modelled in the ZSF. Also for levelling to sea, the measured salt concentration at the depth of the discharge valve is in 89.5% of the events greater than the mean salt concentration at sea. Although this would theoretically lead to a similar underestimation by the ZSF, there is actually an overestimation, potentially caused by the limited measurement resolution in the lock chamber. Due to the relatively short levelling durations, when seawater is entering the lock chamber during levelling, we observe mixing at the first line of CTD-divers but no significant change in salt concentrations at the second line of CTD-divers. This causes the observed salt concentration at the end of the levelling event to be similar to that at the start of the levelling, and hence, to an overestimation of the observed levelling flux by the ZSF. Yet, overall, the performance of the analytical model of the ZSF to predict saltwater intrusion is rewarding, despite the schematic representation of the underlying complex physical processes.

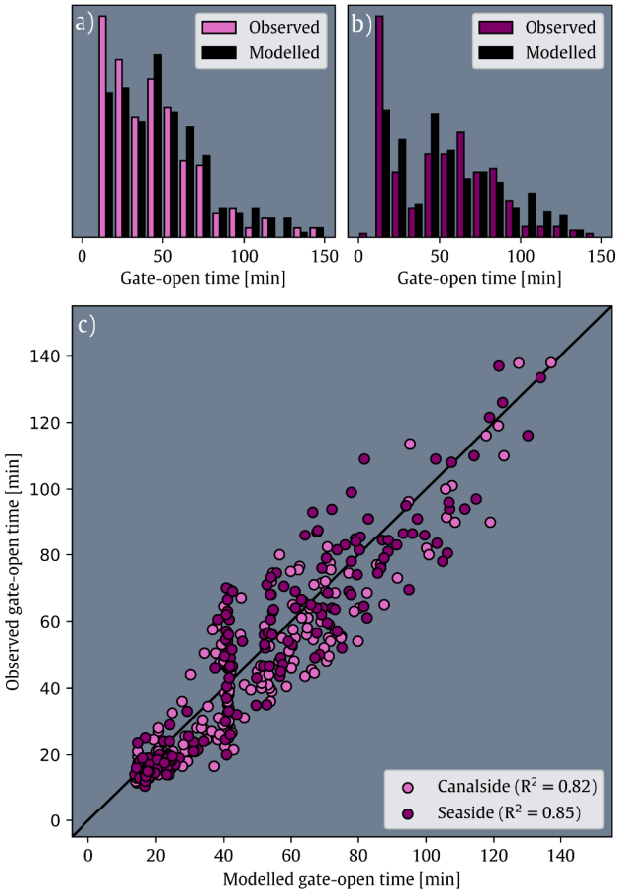

Fig. 8. The distributions of the observed and predicted gate-open durations at **a)** the canal and **b)** the sea; and **c)** the correlation for these distributions.

4.2. *OpenTNSim: The simulated lock operation*

The nautical traffic model yields a distribution of gate-open durations that closely matches the observations (Fig. 8(a) and (b)). The relative error in the cumulative gate-open duration at the canal yields an overestimation of +9.1%, thereby generally underestimating the occurrence of shorter gate-open durations and overestimating the occurrence of longer gate-open durations. This error can be explained by the discrepancies between the modelled and actual lock operation by taking deterministic values instead of stochastic lock operation parameters (Fig. 6). This simplification also leads to mismatches in the decisions of the lock operator on whether to close the last opened gate between two lock operations. In addition, OpenTNSim does not resolve the observed two-way empty lock operations that included gate-open phases to the canal—accounting for 0.9% of the operations; such operations are normally not required to handle nautical traffic. Nevertheless, the nautical traffic model correctly resolves 33 events where the gates at the canalside are closed in between operations, corresponding to 75.0%, while incorrectly modelling 4 extra events and missing 11 events.

Comparison of the observed and "correctly" modelled gate-open events reveals a satisfactory coefficient of determination R^2 of 0.82 for the duration of the events at the canal, increasing to 0.85 for events at sea (Fig. 8(c)). Absolute errors range up to a shy 35 min, but are smaller than 15 min in 81.5% of the gate-open phases at the canalside. For the shorter gate-open durations—most impactful for reducing saltwater intrusion—the absolute errors range up to 25 min, but are less than 10 min in 78.4% of the events. In addition, although the timing of the gate-open phases at the canal in the model and observations satisfactorily overlap for 79.9%, the timing of the gate-open phases in the model runs is slightly ahead of

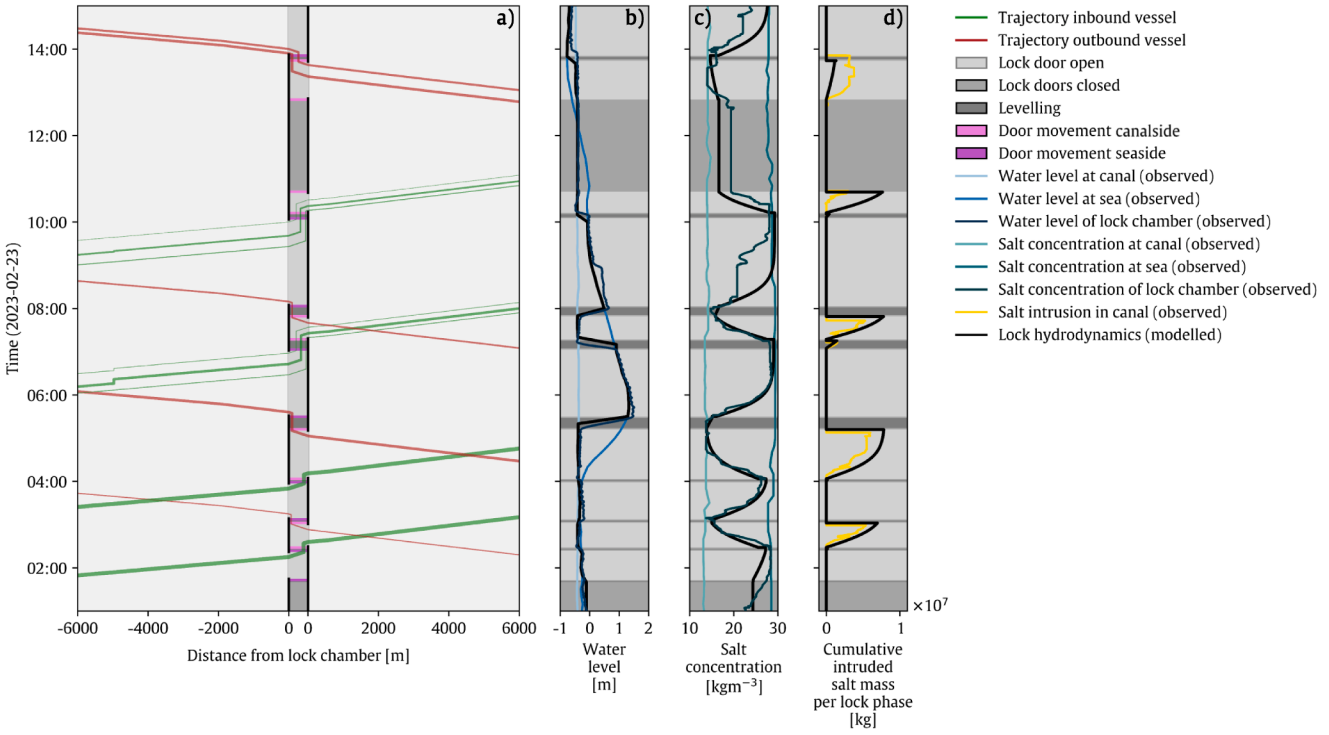

Fig. 9. Results of OpenTNSim–ZSF: **a)** The time-distance diagram of vessels passing the lock (thicker lines indicate larger vessels), **b)** the subsequent predicted water level differences, **c)** salt concentrations, and **d)** intruded salt mass per lock operation phase.

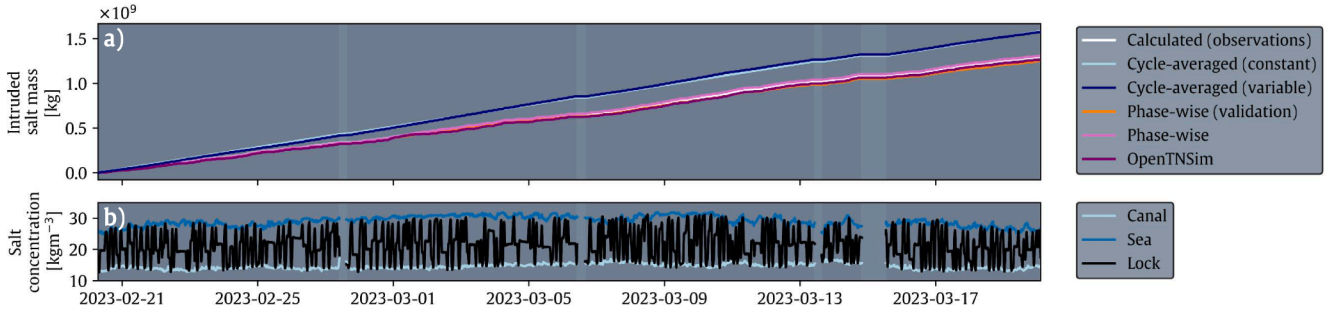

Fig. 10. **a)** comparison of long-term cumulative intruded salt mass for different modelling strategies, excluding the periods of missing data; **b)** the observed salt concentration at sea, the canal, and the lock chamber for reference.

the data. This out-of-phase behaviour is principally caused by a faster levelling process in the model, as it does not yet account for delays due to the mooring of vessels.

The time-distance diagram of vessels passing the lock object in Fig. 9 shows an excerpt of the interaction between the nautical traffic and the lock operation. It shows various lock operations to occur with levelling and gate-open phases of variable durations and vessel occupation rates. Longer gate-open durations are observed to emerge when two subsequent lock operations are planned closely together—when the lock operator generally decides that there is insufficient time to close the gates in between operations—or when multiple vessels have to enter and exit the lock (Fig. 9(a)). The levelling times are visually dependent on the time-varying water level difference between the sea and the canal (Fig. 9(b)).

The corresponding behaviour of the varying salt concentration, calculated with the ZSF using the predicted gate-open duration and vessel volumes by OpenTNSim, is in visual agreement with the observations (Fig. 9(c)). Translating this to salt intrusion mass fluxes (Fig. 9(d)), the density-driven current again appears to be dominant; the long gate-open durations lead to a full exchange of the lock chamber. In addition, the levelling operations towards the canal seem to contribute moderately to this flux when there is a significantly higher water level at sea. Vessels also contribute marginally to the intruded mass flux–i.e., the small peak before the gates close for the outbound operation at 14:00 h (Fig. 9).

4.3. Application: Long-term predicted salt intrusion

Fig. 10 shows the observed long-term salt mass intrusion (white line) and the predictions of each ZSF method application (coloured lines). The rate of the observed intruded salt mass aligns with the frequency of lock operations; during periods of high demand for lockages (i.e., between 03-07 and 03-11 in Fig. 10), more salt intruded over time than during periods of lower demand (i.e., between 03-04 and 03-07 in Fig. 10). Furthermore, there is a minor amplifying effect of an increased salt concentration difference between the sea and the canal. The orange line in Section 4.1 shows the performance of the phase-wise ZSF during validation (i.e., all phases calculated separately with the observed initial salt concentrations in the lock chamber), resulting in the afore-mentioned −3.7% underestimation for the considered period.

When comparing the forecasting performance of the ZSF in its lock cycle-averaged and phase-wise modes, the lock cycle-averaged mode significantly overestimates the measured salt intrusion mass by +22.2% (light blue line in Fig. 10(a)). This discrepancy is the result of the applied average gate-open duration of 63.7 min at the canalside without any calibration factor, causing near-full lock exchanges that are repeated with each lock operation cycle. The distribution of gate-open durations, therefore, appears to significantly reduce salt intrusion, suggesting that shorter gate-open durations are highly impactful. Applying the lock cycle-averaged method with periodically varying lock cycle-averaged environmental conditions (dark blue line in Fig. 10(a)) slightly improves the error, but still leads to an overestimation of +21.5%. Given that the observed long-term salt intrusion mass behaves approximately linearly (white line in Fig. 10(a)), similarly to the predictions of the lock cycle-averaged modes, we can conclude that this mode could capture the long-term salt intrusion mass with sufficient accuracy, provided that representative calibration factors can be derived. In other words, the calibration factors are a must when applying this method. For our case, we calculated that a c_{DOT} of 0.625, effectively reducing the average gate-open duration to a representative gate-open duration equal to 39.8 min, would no longer result in a discrepancy with the observed total salt intrusion mass.

Another notable result is that the (uncalibrated) phase-wise ZSF approach results in a very good match with the observations. An overestimation of only +0.8% is achieved (pink line in Fig. 10(a)) when fully capturing the dynamic frequency in lock operations with varying gate-open durations and external conditions. The error of this phase-wise application is even smaller compared to the run with individual phases for the validation (orange line in Fig. 10(a)). Apparently, the overestimation of saltwater loading at sea and the underestimation of saltwater intrusion in the canal during gate-open phases tend to balance each other out further when using the updated salt concentration of the lock chamber as the initial value for the next phase. It causes the lock chamber to be slightly more saline at the start of gate-open events at the canal, compared to the validation run.

Despite these promising results, we have to recall that the phase-wise application of the ZSF often has limited practical applicability; this method heavily relies on the gate-open durations, which are often unknown or poorly predictable for future scenario analyses. Encouragingly, however, the proposed phase-wise application of the ZSF using OpenTNSim (purple line in Fig. 10(a))—providing gate-open phase information from vessel passage and aggregated lock operation data without the strict necessity of gate-status data (see also Section 5.1)—predicts long-term salt intrusion almost as accurately as the standalone phase-wise application of the ZSF. The coupled model underestimates the long-term intruded salt mass by −2.6%, an increase in error of only 1.8% compared with the purely data-driven phase-wise ZSF application. Like this latter standalone phase-wise application of the ZSF, the coupled model follows the variable rate of saltwater intrusion accurately. The underestimation of the observations of the coupled method can mainly be explained by the underestimation of the occurrence of shorter gate-open durations by OpenTNSim, as explained in Section 4.2.

5. Discussion

Given the new insights into the performance of the ZSF in its application modes and the role of a nautical traffic simulation in supporting its implementation, there are still challenges to further improve its validation (Section 5.1) and application (Section 5.2).

5.1. Improvements for further research

Although the presented method shows very promising results, they are sensitive to the input parameters, For the ZSF in our case study, with substantial gate-open durations, particularly the salt concentrations at sea and at the canalside are sensitive. A 10.0% higher salt concentration at sea would result in 23.5% more saltwater intrusion, while a 10.0% higher salt concentration at the canal would reduce saltwater intrusion by 11.5%. The stronger impact of salt concentration at sea can be attributed to higher water levels at sea relative to the canal, leading to more levelling events with seawater and, consequently, greater salt intrusion. Furthermore, the results show limited sensitivity to vessel dimensions, water levels, and gate-open duration; variations in these parameters lead to changes in saltwater intrusion of an order of magnitude less. The sensitivity for the lock cycle-averaged and phase-wise ZSF modes is similar. Considering OpenTNSim, the gate-open durations are sensitive to the lock operation parameters (i.e., clustering time), but their impact on saltwater intrusion and vessel delays is approximately an order of magnitude smaller. The vessel traffic intensity, leading to more lock operations, is thought to be more influential, although the sensitivity of this was not tested in this study.

Based on the above sensitivities, we highlight the following sources of error that could have affected the quality of the results: measurement uncertainty, model simplifications—both for the ZSF and OpenTNSim library—as well as bias resulting from the specific case study conditions. First, there is uncertainty in the calculated salt intrusion exchange mass fluxes based on the measurements. The main reason for this lies in the limited spatial and depth resolution of the measurement campaign setup. This required a subjective pre-processing analysis to determine the salt mass of the lock chamber. Although the data is highly appreciated and valuable in providing new scientific insights, it only covered the area at the lock gates, rather than along the full length of the lock chamber. This resulted in an artificial step-wise salt mass signal. The change in salt concentration in the lock chamber after gate-opening occurs fast, as the density-driven current reaches the first line of divers close to the opened gate. Then, based on the applied volume-weighting approach, half of the lock chamber is immediately assigned this updated concentration. Subsequently, the exchange flux stagnates as the density-driven current needs time to reach the second line of CTD-divers at the closed gate. Another artificial acceleration of the exchange flux occurs when the density-driven current reaches this second line (see also Fig. 4(d) between 12:30 and 14:00 h). To a lesser extent, this phenomenon also affects the observed change in salt mass caused by the reflected density-driven current.

The restricted measurement resolution also caused the calculated lock chamber-averaged salt concentration from the observations during some gate-open phases to exceed or fall short of the depth-averaged salt concentration at the seaside and canalside, respectively. Moreover, it led to the present internal standing waves with an amplitude of 1.0 kgm^{-3} in the lock chamber to cause significant variability in the average salt concentration over time. This behaviour can clearly be observed when both gates are closed, and the water level is not being levelled (see Fig. 2(d) between 10:30 and 12:30 h). It also seems to affect the estimated salt mass in the initial stage of the density-driven current (i.e., 09:00 and 09:30 h). In addition, the combination of five CTD-divers over the depth, with a slight bias towards deeper waters (Fig. 2(c)), and stratification could have resulted in higher observed salt concentrations, underestimating the observed salt exchange fluxes.

Likewise, the salt concentrations at the sea and canalside may also contain errors, potentially introducing significant biases in the predictions of ZSF. The lock exchange fluxes, in particular the density-driven currents, temporarily change the salt concentration at these harbours, as the lines of CTD-divers were located at a short distance from the lock chamber in the outer and inner harbours. Despite the extensive pre-processing of these concentrations (i.e., removing periods when water is discharged from the lock chamber), the exchange currents have likely affected the salt concentrations at sea and in the canal, causing them to be underestimated and overestimated, respectively. This could result in a general underestimation of the calculated total intruded salt mass. Together with the earlier described challenges in determining the salt

concentration in the lock chamber accurately (Section 4.1), this could explain the scatter in the validation data points in Fig. 7. Although the pre-processing of the lock chamber's salt concentration was designed to reduce the impact of the observation errors on the determined salt mass exchange fluxes, it is estimated that errors up to 3.0 kgm^{-3} in the determination of the initial or final salt concentrations of each phase could have occurred. The limited resolution may have caused observation errors on the order of $2 \cdot 10^6$ kg of saltwater intrusion per phase, equalling up to 25.0% of the lock chamber's salt intrusion capacity. To resolve this, new measurement campaigns with more resolution and a more sophisticated pre-processing could be set up, resulting in a better validation of the ZSF. Recall that the measurement campaign's objective was to study nautical procedures in relation to the hydrodynamic forces (see Section 2.2) rather than to quantify saltwater intrusion.

Second, although the idealised algorithms of the ZSF model resulted in an accurate long-term salt intrusion mass flux, they are also expected to contribute to the discrepancies with the observations. In particular, the neglect of stratification in the method is of concern, as strong stratification is observed from the measurement data. The stratification can increase the speed of the density-driven current (Biemond and Labeur, 2026), which may explain the errors in modelled saltwater exchange due to density-driven currents in this study. Stratification may furthermore cause the return currents of entering and exiting vessels to result in exchange currents of smaller magnitude than those calculated with the ZSF. As there is stronger stratification at the canalside than at the seaside, this may also explain the different discrepancies during the gate-open phase between both harbours. During the levelling phases towards the canal, stratification may have resulted in underestimation of the salt intrusion fluxes, given that the levelling valves are located below the pycnocline. Therefore, we advise further research into including stratification in the ZSF when this would not significantly increase computational times. For example, additional site-dependent calibration factors could be introduced.

Third, the nautical traffic model within the OpenTNSim library could be further validated and improved to more accurately simulate the behaviour of the lock operator, lock master, and the vessels. Although the model provided accurate gate-open durations and vessel traffic delays, we discovered that certain nautical traffic processes and aspects of lock operator behaviour were not included. The following delays could be built into the simulation library to improve the results in gate-open duration distribution:

1. vessel size-dependent sailing-in velocities,
2. vessel size-dependent arrival time gaps,
3. time gaps between the arrival of the last vessel in the lock chamber and the start time of gate-closure,
4. time gaps between the start of levelling after gate-closure,
5. time gaps between the start of the gate-opening after levelling,
6. time gaps between gate-opening and the time the first vessel can demoor; and
7. time gaps between demooring of vessels.

Also, instead of deterministic input parameters, rule-based or stochastic values could be supported. This may prevent unrealistic situations from occurring in the model. For example, while the time of gate-opening in advance of a vessel arrival could be reduced in the simulation, it can, in reality, lead to unsafe situations. In addition, more sophisticated (non-*First-Come-First-Serve*) lock operation planning and (two-dimensional bin packing) vessel positioning algorithms can be added. We also recommend further research on the validation of nautical traffic models such as OpenTNSim, using AIS and lock operation data.

Last, this study only considered Sea Lock IJmuiden, which could be a limitation for the generalisation of the obtained results. Nevertheless, we expect comparable results across lock complexes with different layouts, nautical traffic fleets and intensities, and hydrodynamic forcing conditions. This is due to the density-driven current generally being the dominant process for the amount of saltwater intrusion (Weiler et al., 2026). For example, even an extremely high vessel-occupied lock chamber—with vessels occupying 80.0% of the length, 80.0% of the width, and 90.0% of the depth (i.e., 10.0% under-keel clearance)—would still leave 42.4% of the lock chamber's water volume available to be exchanged through density-driven currents. Furthermore, the applicability of the ZSF is expected to be independent of the hydrodynamic conditions of the study area, although analytical models may be most accurate in weakly stratified systems, where the assumption of uniform salt concentrations in the lock chamber and both harbours is most valid. Consequently, higher tidal ranges and smaller salt concentration gradients across the lock complex may improve the accuracy. Nonetheless, the ZSF seems to perform well under stronger stratification, as demonstrated by our case study at IJmuiden. To confirm the above hypotheses, we advise that this study be repeated for other case studies, meaning that future measurement campaigns should preferably be held in lock chambers with different dimensions and forcing conditions.

5.2. Significance of the coupled method in practice

Despite the afore-mentioned shortcomings, the application of the ZSF resulted in satisfactory performance. The method, particularly the phase-wise mode coupled with the nautical traffic model of OpenTNSim, captured the behaviour of the total salt intrusion mass accurately. The coupled method effectively eliminates the requirement for scarce gate-open status data and salt concentration data in the lock chamber for validation purposes. Given this success, we expect it to be useful for accurately forecasting salt intrusion on the operational, tactical, and strategic levels; the method allows for optimisation of the lock operation based on expected saltwater intrusion, ranging from individual lock operations and lock operation strategies during droughts to normal operation strategies.

On the operational-to-tactical level, the (OpenTNSim-driven) phase-wise ZSF method could be preferred over the lock cycle-averaged mode, as it would be able to predict salt intrusion masses per individual lock operation more accurately. First, this phase-wise method can predict realistic gate-open durations for each operation, which is especially useful when there is a wide distribution in inter-arrival time between vessels and traffic load per lock operation. The resulting wide distribution of gate-open durations, including events with short gate-open durations, generally leads to a substantial reduction in the total salt intrusion load. Second, the phase-wise method predicts variable vessel occupancy in the lock chamber, despite being a second-order effect on the total intruded salt load. On this short timescale, application of the cycle-averaged mode with a calibration factor is less appropriate, as averaging the lock operations inevitably leads to discrepancies between model results and observations for individual lock operations. Furthermore, the description of the operation with a representative gate-open duration typically involves calibration against a larger series of lock cycles, containing all the variations between individual lockages.

An additional benefit of the coupled phase-wise method is that OpenTNSim is capable of estimating vessel delays. With the predicted gate-open durations and occupied lock chamber volume by vessels per lock phase, the simultaneous impact on vessel delays and saltwater intrusion masses (through the ZSF) can be quantified. This would allow for a multi-objective Pareto-optimisation of the short-term lock operation planning—i.e., reducing saltwater intrusion without causing significantly longer vessel delays. Already supported examples are reducing the number of lock operations by clustering vessels in the same lock operation based on maximum waiting times, and shortening gate-open durations through reduced gaps between vessel movements and gate operations (Bakker and van Koningsveld, 2025). Further research could focus on more intelligent queueing and lock operation initiation methods, considering the above trade-off between vessel delays and saltwater intrusion. Machine learning algorithms could add to this analysis, as they can go beyond intuitive or conventional lock operation plan-

ning methods. Thus, the method could automatically identify a series of favourable lock operations, which can be followed by the lock masters and operators, and communicated proactively to vessels, so that these vessels can modify their sailing speed, arriving just-in-time, saving on fuel costs while reducing emissions.

Furthermore, the coupled ZSF–OpenTNSim method could be used to test various longer-term, rule-based lock operation regimes, enabling comprehensive management of the freshwater system. This is particularly useful as adaptation times of salt in the canal system are substantial (Biemond et al., 2024), and lock masters and operators would favour simple operation strategies. For this, trade-off curves can be derived between a lock operation strategy design parameter—i.e., clustering time—and stakeholder performance indicators—i.e., vessel delays and freshwater availability—derived through stakeholder engagement (Bakker et al., 2025). Given that the near-field source terms of salt mass in the canal may not scale linearly to far-field saltwater intrusion—i.e., increased salt concentrations at locations where freshwater is extracted or where saltwater impacts socio-economic or ecological values—quantifying freshwater availability typically requires using numerical models. Numerical models can assess the exceedance of salt concentration limits at important locations in the system (see Fig. 1), using boundary conditions of upstream incoming freshwater, downstream incoming saltwater (from the coupled ZSF–OpenTNSim model), local freshwater extractions and discharges, and flushing discharges. Here, preferably, a faster numerical model should be used to be able to calculate various strategies, such as Biemond et al. (2024). In addition, machine learning methods can be employed to emulate numerical models or construct a data-driven saltwater intrusion model relating the above freshwater and saltwater discharges to the saltwater intrusion length. Additionally, these methods can be employed to rapidly identify Pareto-optimal lock-operation strategies, avoiding the need to explicitly simulate all possible combinations of lock operation strategy design parameters. This could significantly contribute to a digital twin, informing real-time decision support on whether there is a need for extra measures to limit saltwater intrusion (i.e., shifting towards a stricter lock operation regime). In the example of the NSC–ARC system, such method capabilities could be integrated into the existing digital twin,[2] which includes historical and real-time chloride concentration data of measurement buoys.

At a strategic level—when quantifying the impact of new lock chambers, changing environmental conditions, and evolving vessel fleets (in terms of both vessel dimensions and traffic intensities) on the total saltwater intrusion mass—it is debatable whether the coupled method could be of benefit. As the added complexity of developing a phase-wise method coupled to a nautical traffic model—requiring vessel-traffic data processing, detailed lock-operation strategy information, and extrapolation to future conditions—may not outweigh the practicality of a lock cycle-averaged ZSF run. However, for this, the most critical step is to obtain a plausible calibration factor. For now, this highly sensitive factor can only be derived using cross-model comparison with a phase-wise ZSF model, requiring gate status data. When data on gate-open durations is missing—i.e., for new lock complexes/chambers—or when nautical traffic intensifies, or vessel sizes are increasing, the calibration factor can no longer be accurately derived. This could lead to misestimations in the total saltwater intrusion masses, as demonstrated in this study. To determine this calibration factor in these cases, the nautical traffic model of OpenTNSim could be useful. Further research could therefore focus on the derivation of the calibration factor prior to simulation with the ZSF.

[2] https://www.arcgis.com/home/item.html?id=fd64fe585cd240599360f45458e97f68

6. Conclusion

This paper identified a knowledge gap regarding the uncertainty in estimating saltwater intrusion mass fluxes through navigation locks, which pose challenges for freshwater supply during droughts. Considering a case study of Sea Lock IJmuiden in the Netherlands, for which gate-status data, water level and salt concentration measurements, and vessel passage records were available for a month, we found that analytical lock exchange models can accurately estimate observed long-term cumulative salt intrusion mass fluxes. Validation of the Sea Lock Formulation (*in Dutch: Zeesluisformulering*, ZSF) model, considering all lock operation phases individually using observed initial conditions, resulted in a minor underestimation of the cumulative salt intrusion mass by −3.7%. However, when applying the model—where each calculation starts from the last determined salt concentration in the lock chamber—the accuracy strongly depends on the availability of lock phase-specific data, such as gate-status data. For our case, assuming phase-specific data would be unavailable and subsequently a lock cycle-averaged run with ZSF would have to be ran without prior site-specific calibration, the model overestimated the total observed saltwater intrusion mass flux by +22.2%. When phase-specific data is available, calibration factors can be determined with the ZSF by simulating lock operations in a phase-wise mode with phase-varying gate-open durations, resulting in a significant improvement in estimation of the cumulative saltwater intrusion mass flux to an error of +0.8%.

To provide the ZSF with realistic phase-varying gate-open durations when these data are unavailable (e.g., for forecasting purposes), we coupled the ZSF with a nautical traffic simulation model using the OpenTNSim-library, which includes a locking module. For this, it uses actual nautical traffic from widely accessible sources, such as AIS, and deterministic lock operation parameters that closely reproduce the behaviour of the lock operator. Application of this coupled method resulted in an underestimation of the cumulative saltwater intrusion by −2.6%. The slightly poorer performance compared to the hindcasted standalone phase-wise application of the ZSF can largely be attributed to the underestimation of the shorter gate-open durations at the canal. This is caused by missing nautical processes that can be flexibly added to the open-source library in future research.

Despite resolvable shortcomings, the coupled method proved a significant step forward in accurately modelling saltwater intrusion through navigation locks. An additional benefit of using OpenTNSim is the simultaneous estimation of vessel delays. We therefore foresee that the coupled method can be applied in practice to optimise lock design and operation strategies that jointly limit saltwater intrusion and vessel delays. Thereby, the method is highly suitable to be adopted to generate realistic boundary conditions for hydrodynamic models that can predict saltwater intrusion lengths in the canal. Thus, we facilitate a first step in the urgently needed method that enables quantification of the risk of freshwater shortages and economic losses for waterborne transport in closed systems in times of rapid socioeconomic developments and climate change effects.

Funding

This research is financially supported by SmartPort, which is a collaboration between the Port of Rotterdam, universities, institutes and companies in the Dutch ports and waterways sector.

Data availability

The underlying measurement data is subject to third-party restrictions of Deltares. Requests can be made to A.J.v.d.H.

CRediT authorship contribution statement

Floor P. Bakker: Writing – original draft, Visualization, Validation, Supervision, Software, Methodology, Investigation, Formal analysis, Data curation, Conceptualization; **Jikke W.E. de Ruiter:** Validation, Methodology, Investigation, Formal analysis, Data curation, Conceptualization; **Arne J. van der Hout:** Writing – review & editing, Resources, Methodology, Data curation, Conceptualization; **Mark van Koningsveld:** Writing – review & editing, Supervision, Software, Project administration, Methodology, Funding acquisition, Conceptualization.

Declaration of competing interest

The authors declare the following financial interests/personal relationships which may be considered as potential competing interests:

Mark van Koningsveld reports financial support was provided by SmartPort. Arne van der Hout reports a relationship with Deltares that includes: employment. Mark van Koningsveld reports a relationship with Van Oord NV that includes: employment. If there are other authors, they declare that they have no known competing financial interests or personal relationships that could have appeared to influence the work reported in this paper.

Acknowledgements

The authors want to thank Deltares for making available the measurement data of this paper and for the open-source software development of the analytical lock exchange model of the Sea Lock Formulation (in Dutch: *Zeesluisformulering*). The open-source nature of this software greatly enhances transparency, reproducibility, and wider community use. Specifically, we extend our thanks to Otto Weiler, who laid the foundation of the Sea Lock Formulation, for his suggestions that improved our work.

References

Abraham, G., Van der Burgh, P., 1964. Pneumatic reduction of salt intrusion through locks. J. Hydraul. Div. 90 (1), pp. 83—119. https://doi.org/10.1061/JYCEAJ.0001009.

Abraham, G., Van der Burgh, P., De Vos, P., 1973. Pneumatic Barriers to Reduce Salt Intrusion Through Locks. Technical Report. Rijkswaterstaat.

Baart, F., Jiang, M., Bakker, F.P., Van Gijn, M., Frijlink, T., Van Koningsveld, M., 2022. OpenTNSim. https://doi.org/10.5281/zenodo.7053274.

Bakker, F.P., Baart, F., van Koningsveld, M., 2024. OpenTNSim version v1.4.0-paper.3. https://doi.org/10.5281/zenodo.11489436.

Bakker, F.P., Hendricks, G.G., Keyzer, L.M., Iglesias, S.R., Aarninkhof, S.G.J., van Koningsveld, M., 2025. Trading off dissimilar stakeholder interests: changing the bed level of the main shipping channel of the rhine-meuse delta while considering freshwater availability. Environ. Challenges. https://doi.org/10.1016/j.envc.2025.101323

Bakker, F.P., van Koningsveld, M., 2025. Optimizing navigation lock operation when climate change strikes. In: IAME Conference 2025 – Bergen.

Bakker, F.P., van Koningsveld, M., Baart, F., van der Werff, S., Kirichek, A., Pourmohammad-Zia, N., in prep. OpenTNSim - analysis of traffic behaviour on networks for different traffic scenarios and network configurations. SoftwareX.

Basser, H., Rudman, M., Daly, E., 2017. SPH modelling of multi-fluid lock-exchange over and within porous media. Adv. Water Res. 108, 15–28. https://doi.org/10.1016/j.advwatres.2017.07.011

Battiston, C.C., Bombardelli, F.A., Schettini, E.B.C., Marques, M.G., 2020. Mean flow and turbulence statistics through a sluice gate in a navigation lock system: a numerical study. Eur. J. Mech. - B/Fluids 84, 155–163. https://doi.org/10.1016/j.euromechflu.2020.06.003

Benjamin, T.B., 1968. Gravity currents and related phenomena. J. Fluid Mech. 31 (2), 209—248. https://doi.org/10.1017/S0022112068000133

Biemond, B., Labeur, R.J., 2026. Adjustment time of the lock exchange for a linearly stratified lock and ambient. Environ. Fluid Mech. 26 (9). https://doi.org/10.1007/s10652-026-10073-5

Biemond, B., Vuik, V., Lambregts, P., de Swart, H.E., Dijkstra, H.A., 2024. Salt intrusion and effective longitudinal dispersion in man-made canals, a simplified model approach. Estuarine, Coastal Shelf Sci. 298 (108654). https://doi.org/10.1016/j.ecss.2024.108654

Bombardelli, F.A., Cantero, M.I., Garcia, M.H., Buscaglia, G.C., 2009. Numerical aspects of the simulation of discontinuous saline underflows: the lock-exchange problem. J. Hydraul. Res. 47 (6), 777–789. https://doi.org/10.3826/jhr.2009.3238

Buschman, F.A., Tiessen, M., 2017. Zoutverspreiding in het Noordzeekanaal en Amsterdam-Rijnkanaal. Analyse van 100-Punten-Metingen. Technical Report 11200589-001-ZWS-0004. Deltares. https://publications.deltares.nl/11200589_001a.pdf.

Calvo Gobbetti, L.E., 2013. Design of the filling and emptying system of the new panama canal locks. J. Appl. Water Eng. Res. 1. https://doi.org/10.1080/23249676.2013.827899

Chen, S.-N., Geyer, W.R., Ralston, D.K., Lerczak, J.A., 2012. Estuarine exchange flow quantified with isohaline coordinates: contrasting long and short estuaries. J. Phys. Oceanogr. 42 (5), 748–763. https://doi.org/10.1175/JPO-D-11-086.1

Constantinescu, G., 2014. Les of lock-exchange compositional gravity currents: a brief review of some recent results. Environ. Fluid Mech. , 295—317. https://doi.org/10.1007/s10652-013-9289-0

de Fockert, A., O'Mahoney, T.S.D., Nogueira, H.I.S., Oldenziel, G., Bijlsma, A.C., Janssen, H., 2022. Assessing the effectiveness of the IJmuiden salt screen design for nonuniform selective withdrawal by physical and numerical modeling. J. Hydraul. Eng. 148. https://doi.org/10.1061/(ASCE)HY.1943-7900.0001958

De Groot- Wallast, I., Vreeken, T., 2016. Validatierapport WANDA-Locks, Het Nieuwe Zoutlekmodel. Technical Report. Deltares. https://publications.deltares.nl/1209463_000.pdf.

De Loor, A., Van der Hout, J., Weiler, O.M., Kortlever, W.C.D., 2013. The use and validation of openFOAM to determine the lateral and longitudinal forces exerted on a vessel in the lock and in the lock approach. In: International Conference on Ship Manoeuvring in Shallow and Confined Water: with nonexclusive focus on Ship Behaviour in Locks, pp. 157—166.

Deltares, 2023. Dichtheidsmetingen Zeesluis IJmuiden 2023. Technical Report 11209319-000-HYE-0002. Report prepared by Van der Hout, A.

Geyer, W.R., Ralston, D.K., Chen, J.-L., 2005. Mechanisms of exchange flow in an estuary with anarrow, deep channel and wide, shallow shoals. JGR Oceans 65 (4), 607–624. https://doi.org/10.1029/2020JC016092DigitalObjectIdentifier(DOI)

Ghasemi V. , A., Firoozabadi, B., Mahdinia, M., 2013. 2D numerical simulation of density currents using the SPH projection method. Eur. J. Mech. - B/Fluids 38, 38–46. https://doi.org/10.1016/j.euromechflu.2012.10.004

Ha, J.H., Gourlay, T., 2017. Bow and stern sinkage coefficients for cargo ships in shallow open water. PIANC Yearbook 2017.

Hatcher, T.M., Manoj, K.C., Vasconcelos, J.G., Fang, X., 2012. A comparison between numerical modeling approaches for the simulation of gravity currents. In: World Environmental and Water Resources Congress 2012, pp. 1108–1118. https://doi.org/10.1061/9780784412312.113

Hatcher, T.M., Vasconcelos, J.G., 2013. Finite-volume and shock-capturing shallow water equation model to simulate boussinesq-type lock-exchange flows. J. Hydraul. Eng. 139. https://doi.org/10.1061/(ASCE)HY.1943-7900.0000775

Hendriks, D., Mens, M., 2023. De droogte van 2022: EEN Brede Analyse van de ernst en maatschappelijke gevolgen, Achtergrondrapport. Technical Report. Deltares, KWR, WUR, WER, KnowH2O.

Henn, R., 2013. Real-time simulation of ships manoeuvring in locks. In: 3rd International Conference on Ship Manoeuvring in Shallow and Confined Water: With Non-Exclusive Focus on Ship Behaviour in Locks. R.I.N.A., pp. 215—219.

Härtel, C., Kleiser, L., Michaud, M., Stein, C.F., 1997. A direct numerical simulation approach to the study of intrusion fronts. J. Eng. Math. 32, 103—120. https://doi.org/10.1023/A:1004215331070

Jirka, G.H., 1979. Supercritical withdrawal from two-layered fluid systems: Part 1 - two-dimensional skimmer wall. Hiyrbak if Hydraul. Res. 17, 43–51. https://doi.org/10.1080/00221687909499599

Jirka, G.H., Katavola, D.S., 1979. Supercritical withdrawal from two-layered fluid systems: Part 2 -. Hiyrbak if Hydraul. Res. 17, 53–62. https://doi.org/10.1080/00221687909499600

Jones, E.R., Bierkens, M. F.P., van Vliet, M. T.H., 2024. Current and future global water scarcity intensifies when accounting for surface water quality. Nat. Climate Change , 1–7https://doi.org/10.1038/s41558-024-02007-0

Jongeling, T.H.G., 2003. Salt Water Intrusion Analysis Panama canal Locks. Existing situation. Report A: Field Data Collection, Development and Validation of Simulation Model, Analysis of Salt Water Intrusion. Technical Report Q3039. WL|Delft Hydraulics.

Jongeling, T.H.G., 2004. Salt Water Intrusion Analysis Panama Canal Locks. Future situation: Post-Panamax Locks. Reports E. Part I: Effect of water Recycling at Pacific Side of Canal, Part II: Alternative Methods to Mitigate Salt Water Intrusion. Technical Report Q3476. WL|Delft Hydraulics.

Jongeling, T.H.G., 2008. Water Quality Model of Gatun Lake for Expanded Panama Canal. Part III Water Quality Monitoring. Technical Report Q3959. Deltares.

Kao, T.W., Park, C., Pao, H.P., 1977. Buoyant surface discharge and small-scale oceanic fronts: a numerical study. JGR Oceans Atmos. 82, 1747–1752. https://doi.org/10.1029/JC082i012p01747

Keetels, G., Uittenbogaard, R., Cornelisse, H., Villars, N., Van Pagee, H., 2011. Field study and supporting analysis of air curtains and other measures to reduce salinity transport through shipping locks. Irrig. Drain.. https://doi.org/10.1002/ird.679

Kerstma, J., Kolkman, P.A., Regeling, H.J., Venis, W.A., 1994. Water Quality Control at Ship Locks: Prevention of Salt- and Fresh Water Exchange. 158561, Balkema.

Keulegan, G.H., 1957. Thirteenth Progress Report on Model Laws for Density Currents; An Experimental Study of the Motion of Saline Water from Locks into Fresh Water Channels. Technical Report. U.S. National Bureau of Standards. Washington, D.C.

Kim, C.-K., Park, K., 2012. A modeling study of water and salt exchange for a micro-tidal, stratified northern gulf of mexico estuary. J. Mar. Syst. 96-97, 103–115. https://doi.org/10.1016/j.jmarsys.2012.02.008

Kolar, R.L., Kibbey, T.C.G., Szpilka, C.M., Dresback, K.M., Tromble, E.M., Toohey, I.P., Hoggan, J.L., Atkinson, J.H., 2009. Process-oriented tests for validation of baroclinic shallow water models: the lock-exchange problem. Ocean Model. 28 (1), 137–152. The Sixth International Workshop on Unstructured Mesh Numerical Modelling of Coastal, Shelf and Ocean Flows. https://doi.org/10.1016/j.ocemod.2009.01.003

Lai, Z., Chen, C., Cowles, G.W., Beardsley, R.C., 2010. A nonhydrostatic version of FVCOM: 1. Validation experiments. JGR Oceans. https://doi.org/10.1029/2009JC005525
Lee, J., Biemond, B., de Swart, H., Dijkstra, H.A., 2024. Increasing risks of extreme salt intrusion events across European estuaries in a warming climate. Commun. Earth Environ. 5 (60). https://doi.org/10.1038/s43247-024-01225-w
Lesshafft, L., Meiburg, E., Kneller, B., Marsden, A., 2011. Towards inverse modeling of turbidity currents: the inverse lock-exchange problem. Comput. Geosci. 37 (4), 521–529. https://doi.org/10.1016/j.cageo.2010.09.015
Lindberg, O., Glimberg, S.L., Bingham, H.B., Engsig-Karupf, A.P., Schjeldahl, P.J., 2013. Real-time simulation of ship-structure and ship-ship interaction. In: 3rd International Conference on Ship Manoeuvring in Shallow and Confined Water: With Non-Exclusive Focus on Ship Behaviour in Locks. R.I.N.A, pp. 257—264.
MacCready, P., Geyer, W.R., Burchard, H., 2018. Estuarine exchange flow is related to mixing through the salinity variance budget. J. Phys. Oceanogr. 48 (6), 1375–1384. https://doi.org/10.1175/JPO-D-17-0266.1
Marin, M., Zhu, Y., Andrade, L.A., Atencio, E., Boya, C., Mendizabal, C., 2010. Supply chain and hybrid modeling: the panama canal operations and its salinity diffusion. In: Proceedings of the 2010 Winter Simulation Conference, pp. 2023–2033. https://doi.org/10.1109/WSC.2010.5678869
Mausshardt, S., Singleton, G., 1995. Mitigating salt-water intrusion through Hiram M. Chittenden locks. J. Waterways, Port, Coastal, Ocean Eng. 121, 224–227. https://doi.org/10.1061/(ASCE)0733-950X(1995)121:4(224)
Mucha, P., 2025. CFD analysis of ships entering locks. In: MARINE 2025 - XI International Conference on Computational Methods in Marine Engineering.
Oldeman, A.M., Kamath, S., Masterov, M.V., O'Mahoney, T.S.D., van Heijst, G.J.F., Kuipers, J.A.M., Buist, K.A., 2020. Numerical study of bubble screens for mitigating salt intrusion in sea locks. Int. J. Multiphase Flow 129 (103321). https://doi.org/10.1016/j.ijmultiphaseflow.2020.103321
O'Mahoney, T.S.D., De Jonge, M., Boeters, R., Vreeken, T., 2023. Innovative salt-freshwater separation system at the krammer locks, the netherlands. Hydraulic modelling to balance functional requirements. In: Proceedings of PIANC Smart Rivers 2022, pp. 479—493.
O'Mahoney, T.S.D., Oldenziel, G., van der Ven, P., 2024. The effect of bubble size on lock-exchange density currents through bubble screens. J. Hydraul. Eng. 150. https://doi.org/10.1061/JHEND8.HYENG-13531
Ottolenghi, L., Prestininzi, P., Montessori, A., Adduce, C., La Rocca, M., 2018. Lattice Boltzmann simulations of gravity currents. Eur. J. Mech. - B/Fluids 67, 125–136. https://doi.org/10.1016/j.euromechflu.2017.09.003
Parchure, T.M., Wilhelms, S.C., Sarruff, S., McAnally, W.H., 2000. Salinity Intrusion in the Panama Canal. Technical Report. U.S. Army Engineer Research and Development Center. https://doi.org/10.21236/ADA378475
Pelmard, J., Norris, S., Friedrich, H., 2018. Les grid resolution requirements for the modelling of gravity currents. Comput. Fluids 174, 256–270. https://doi.org/10.1016/j.compfluid.2018.08.005
PIANC, 1986. Final Report of the International Commission for the Study of Locks. Technical Report. PIANC - The World Association for Waterborne Transport Infrastructure.
PIANC, 2021. Saltwater Intrusion Mitigation in Inland Waterways. Technical Report InCom WG Report 198. PIANC - The World Association for Waterborne Transport Infrastructure.
Pozorski, J., Olejnik, M., 2023. Smoothed particle hydrodynamics modelling of multiphase flows: an overview. Acta Mech. 235, 1–30. https://doi.org/10.1007/s00707-023-03763-4
Rabelo, L., Cruz, L., Bhide, S., Joledo, O., Pastrana, J., Xanthopoulos, P., 2014. Analysis of the expansion of the panama canal using simulation modeling and artificial intelligence. In: Proceedings of the Winter Simulation Conference 2014, pp. 910–921. https://doi.org/10.1109/WSC.2014.7019951
Rijkswaterstaat, 2023. Operationeel watermanagement Amsterdam-Rijnkanaal en Noordzeekanaal. WVL0723ZB174A. https://iplo.nl/thema/water/beheer-watersysteem/infographics-operationeel-watermanagement/.
Rossa, A.L., Coutinho, A.L.G.A., 2013. Parallel adaptive simulation of gravity currents on the lock-exchange problem. Comput. Fluids 88, 782–794. https://doi.org/10.1016/j.compfluid.2013.06.008
Shao, S., 2011. Incompressible smoothed particle hydrodynamics simulation of multifluid flows. Numer. Methods. Fluids. https://doi.org/10.1002/fld.2660
Stancanelli, L.M., Musumeci, R.E., Foti, E., 2018. Computational fluid dynamics for modeling gravity currents in the presence of oscillatory ambient flow. Water 10 (635). https://doi.org/10.3390/w10050635
Stockstill, R.L., Berger, R.C., 2009. A three-dimensional numerical model for flow in a lock filling system. In: World Environmental and Water Resources Congress 2009, pp. 1–10. https://doi.org/10.1061/41036(342)278
Thorenz, C., Strybny, J., 2012. On the numerical modelling of filling-emptying system for locks. In: Proceedings of 10th International Conference on Hydroinformatics. Hamburg: TuTech Innovation, Hamburg, Germany, July 14 - 18.
Toxopeus, S.L., Bhawsinka, K., et al., 2013. Calculation of hydrodynamic interaction forces on a ship entering a lock using CFD. In: I4th MASHCON. Bundesanstalt für Wasserbau, Hamburg, pp. 157—166. https://doi.org/10.18451/978-3-939230-38-0_34
Uittenbogaard, R.E., 2010. Voorstudie: Ontwerpstudie en Praktijkproef Zoutlekbeperking Volkeraksluizen. Technical Report. Deltares. https://www.deltaexpertise.nl/images/c/cd/Rapport_01_Voorstudie_en_zoutvrachtberekeningen.pdf.
Uittenbogaard, R.E., Cornelisse, J.M., 2011. Ontwerpstudie en Praktijkproef Zoutlekbeperking Volkeraksluizen - Beschrijving en Resultaten Praktijkproef Stevinsluis en Evaluatie Maatregelen Stevinsluis. Technical Report 1201226-005. Deltares. https://www.deltaexpertise.nl/images/f/f8/Rapport_04_Praktijkproef_Stevinsluis.pdf.
Uittenbogaard, R.E., Cornelisse, J.M., O'Hara, K., 2015. Water - air bubble screens reducing salt intrusion through shipping locks. In: 36th IAHR World Congress, pp. 162–167.
UNESCO, 1981. The Practical Salinity Scale 1978 and the International Equation of State of Seawater 1980. Technical Report 36. UNESCO: United Nations Educational Scientific and Cultural Organization.
van der Burgh, P., de Vos, P., 1962. Luchtschermen in Schutsluizen. Technical Report. Rijkswaterstaat. https://open.rijkswaterstaat.nl/publish/pages/107606/luchtschermen_in_schutsluizen.pdf.
Van Beek, A.H.N., 2021. The Influence of a Flushing Discharge on Lock-Exchange. Master's thesis. Eindhoven University of Technology. https://research.tue.nl/en/studentTheses/the-influence-of-a-flushing-discharge-on-lock-exchange.
van der Hout, A., Schotman, A.D., Kempenaar, R., Kortlever, W.C.D., 2024. Evaluation of hydraulic and nautical performance of sea lock IJmuiden after two years of operation. In: Proceedings of the 35th PIANC World Congres 2024, pp. 1411–1417. https://research.tudelft.nl/en/publications/evaluation-of-hydraulic-and-nautical-performance-of-sea-lock-ijmu/.
Van der Kuur, P., 1985. Locks with devices to reduce salt intrusion. J. Waterway, Port, Coastal Ocean Eng. 111 (6). https://doi.org/10.1061/(ASCE)0733-950X(1985)111:6(1009)
van der Ven, P., O'mahoney, T., Weiler, O., 2018. Methods to assess bubble screens applied to mitigate salt intrusion through locks. In: Proceedings of the 34th PIANC World Congress 2018.
van Koningsveld, M., den Uijl, J.A.W., 2019. OpenTNSim (Version 0.0.1). https://doi.org/10.5281/zenodo.3341517 software.
Vergote, T., Eloot, K., Vantorre, M., Verwilligen, J., 2013. Hydrodynamics of a ship while entering a lock. In: 3rd International Conference on Ship Manoeuvring in Shallow and Confined Water: with non-exclusive focus on Ship Behaviour in Locks. R.I.N.A., pp. 281–289.
Vinke, F., Turpijn, B., van Gelder, P., van Koningsveld, M., 2024. Inland shipping response to discharge extremes - A 10 years case study of the Rhine. Climate Risk Manage. 43, 100578. https://doi.org/10.1016/j.crm.2023.100578
Vinke, F., van Koningsveld, M., van Dorsser, C., Baart, F., van Gelder, P., Vellinga, T., 2022. Cascading effects of sustained low water on inland shipping. Climate Risk Manage. 35, 100400. https://doi.org/10.1016/j.crm.2022.100400
Vrijburcht, A., 1991. Forces on Ships in Navigation Locks Induced by Stratified Flows. Ph.D. thesis. Delft University of Technology.
Vrijburcht, A., 2000a. Design of Locks: Part I. Rijkswaterstaat.
Vrijburcht, A., 2000b. Ontwerp van Schutsluizen. Ministerie van Verkeer en Waterstaat, Rijkswaterstaat, Bouwdienst (RWS, BD). https://open.rijkswaterstaat.nl/@185991/ontwerp-schutsluizen/.
Vuik, V., Lambregts, P., 2023. Verzilting Kanaal Gent-Terneuzen - Rapportage oppervlaktewatermodellering. Technical Report. HKV lijn in water. https://www.vliz.be/imisdocs/publications/392086.pdf.
Wang, H.-Z., Zou, Z.J., 2013. Numerical study on hydrodynamic behaviour of ships sailing in locks. In: 3rd International Conference on Ship Manoeuvring in Shallow and Confined Water: With Non-Exclusive Focus on Ship Behaviour in Locks. R.I.N.A., pp. 129—134.
Wang, H.-Z., Zou, Z.J., 2014. Numerical prediction of hydrodynamic forces on a ship passing through a lock with different lock shape. J. Hydrodyn. 26, 1–9.
Weiler, O., 2018. Zoutindringing Door Schutsluizen, Overzicht Projecten en Aanzet Formulering t.b.v. Netwerkmodellen. Technical Report. Deltares. https://www.nattekunstwerkenvandetoekomst.nl/document/zoutindringing-schut-en-spuisluizen-overzicht-projecten-zoutindringing-door-schutsluizen-en-aanzet-zeesluisformulering/.
Weiler, O., O'Mahoney, T., Burgers, R., 2019. Opzet en verkenning Zeesluisformulering. Technical Report. Deltares. https://www.vstest.nl/wp-content/uploads/2024/05/KpNK-2017-SKW-01c001_KENNISBIJDRAGE_Zoutindringing-door-schut-en-spuisluizen-Overzicht-projecten-en-aanzet-ZSF_DEF-20190326.pdf.
Weiler, O.M., Vreeken, T., Maijvis, S.D., Zuiderwijk, N.L., O'Mahoney, T.S.D., 2026. Quantification of Salt Intrusion caused by Navigation Locks and their Operation for Policy Analysis, Water Management or Salt Dispersion Modelling. J. Coastal Hydraul. Structures 6 (1). https://doi.org/10.59490/jchs.2026.0052
Wijsman, J., 2013. Panama Canal Extension: A Review on Salt Intrusion into Gatun Lake. Technical Report. IMARES Wageningen UR - Institute for Marine Resources & Ecosystem Studies.
Xu, D., Li, Z., An, J., 2023. Water level calculation and influencing factors of single-step locks with water-saving basins. In: Proceedings of PIANC Smart Rivers 2022, pp. 552—564.
Zhao, L., Yu, C.-H., He, Z., 2019. Numerical modeling of lock-exchange gravity/turbidity currents by a high-order upwinding combined compact difference scheme. Int. J. Sediment Res. 34 (3), 240–250. https://doi.org/10.1016/j.ijsrc.2018.10.001
Zhu, L., Wang, X., Huang, Y., Liu, B., Li, Z., 2023. Study on classification arrangement and hydraulic characteristics of water-saving ship lock under ultra-high head. In: Proceedings of PIANC Smart Rivers 2022, pp. 1553–1564.